Supporting Information

All-organic fast intersystem crossing assisted exciplexes exhibiting sub-microsecond thermally activated delayed fluorescence

Kaspars Traskovskis,[a*] Armands Sebris,[a] Irina Novosjolova,[a] Māris Turks,[*a] Matas Guzauskas,[b] Dmytro Volyniuk,[b] Oleksandr Bezvikonnyi,[b] Juozas V. Grazulevicius,[b] Anatoly Mishnev,[c] Raitis Grzibovskis,[d] Aivars Vembris[d]

a Faculty of Materials Science and Applied Chemistry, Riga Technical University, P. Valdena Str. 3, LV-1048, Riga, Latvia.
E-mail: kaspars.traskovskis@rtu.lv, maris.turks@rtu.lv
b Department of Polymer Chemistry and Technology, Kaunas University of Technology, Barsausko 39, LT- 51423, Kaunas, Lithuania.
c Latvian Institute of Organic Synthesis, Aizkraukles Str. 21, Riga LV-1006, Latvia
d Institute of Solid State Physics, University of Latvia, Kengaraga Str. 8, LV-1063, Riga, Latvia.

Contents

Supplementary figures and tables

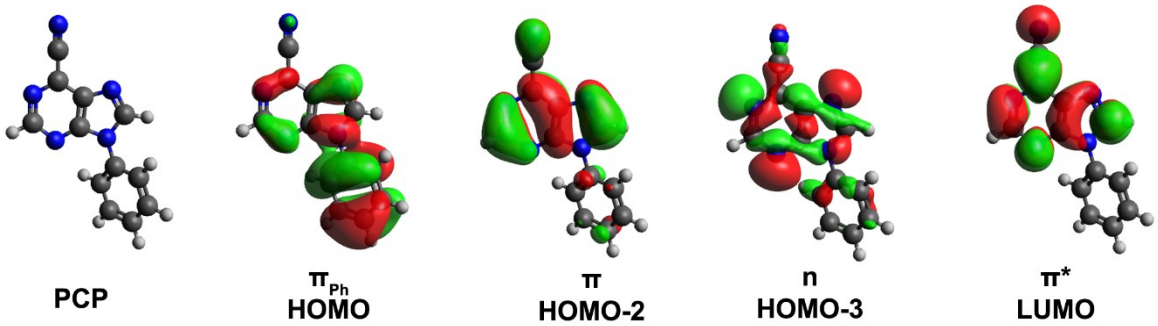

Figure S1. Molecular orbitals of the purine derivatives involved in the lowest energy electronic transitions (M06-2X/6-311G**, ground-state geometry, CPCM solvation in THF).

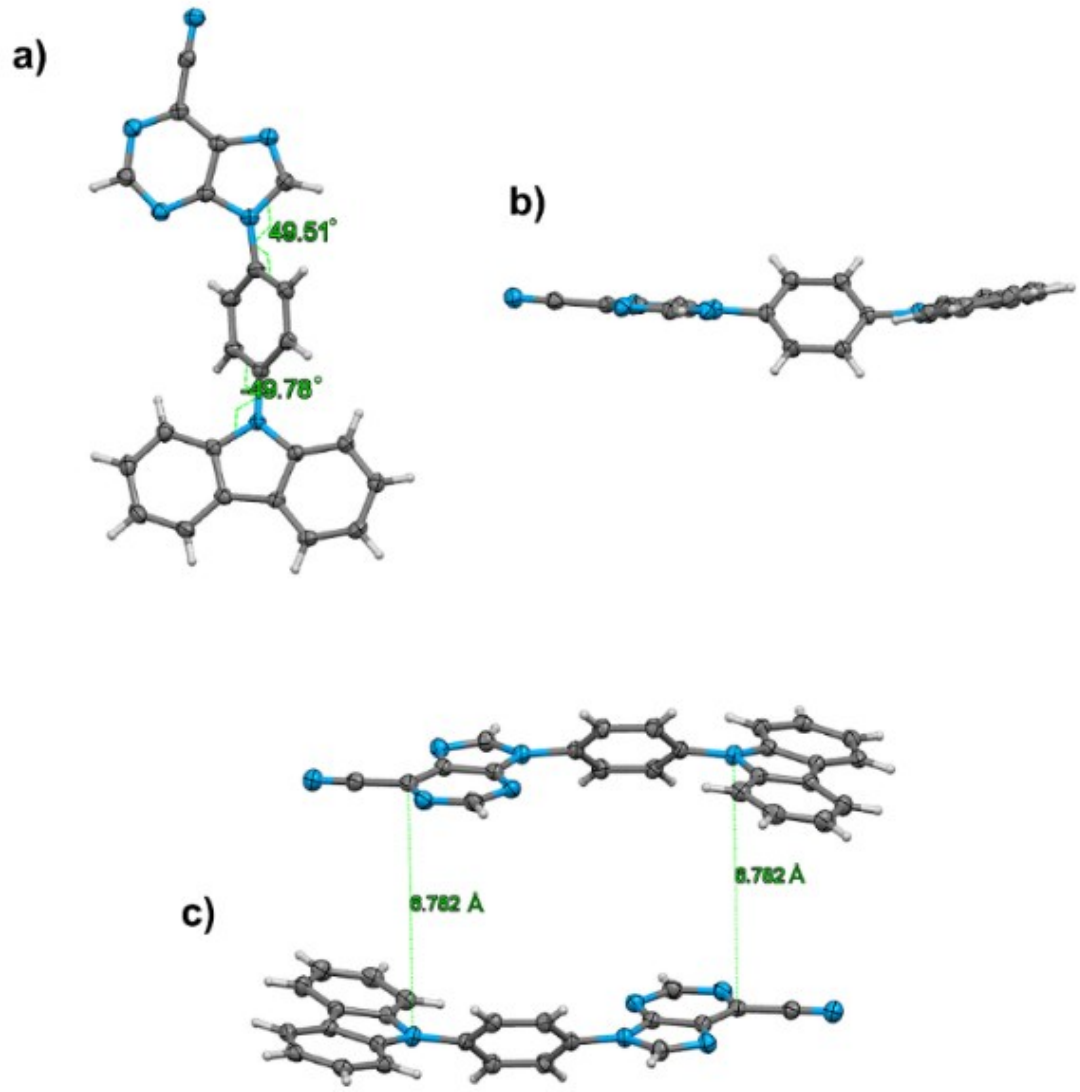

Figure S2. X-ray structure of PCbz-2 with thermal ellipsoids shown at the 50% probability level. (a) Top view; dihedral angles between central phenyl ring and D and A fragments are indicated. (b) Side view. (c) Packing pattern of the neighbouring molecules.

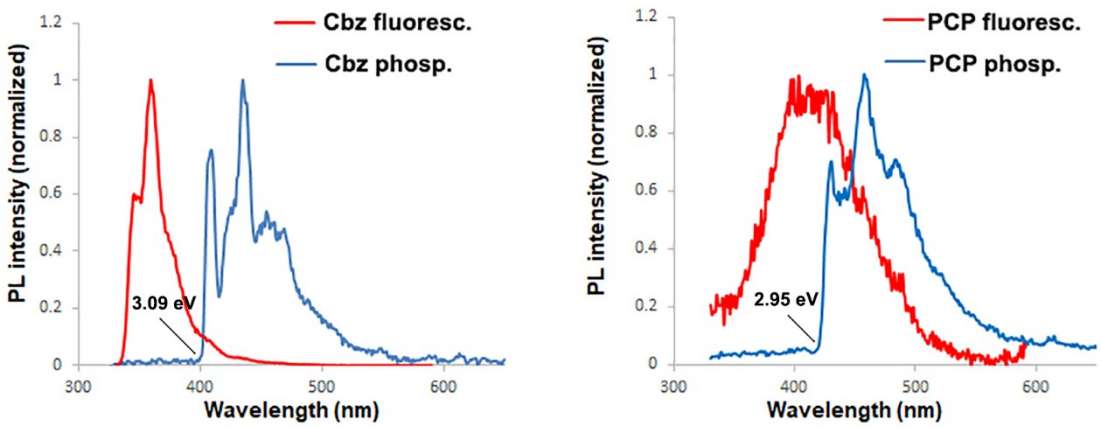

Figure S3. Fluorescence (0-50 μs) and phosphorescence (50-5000 μs) emission bands of Cbz and PCP, measured in 2-MeTHF at 77 K.

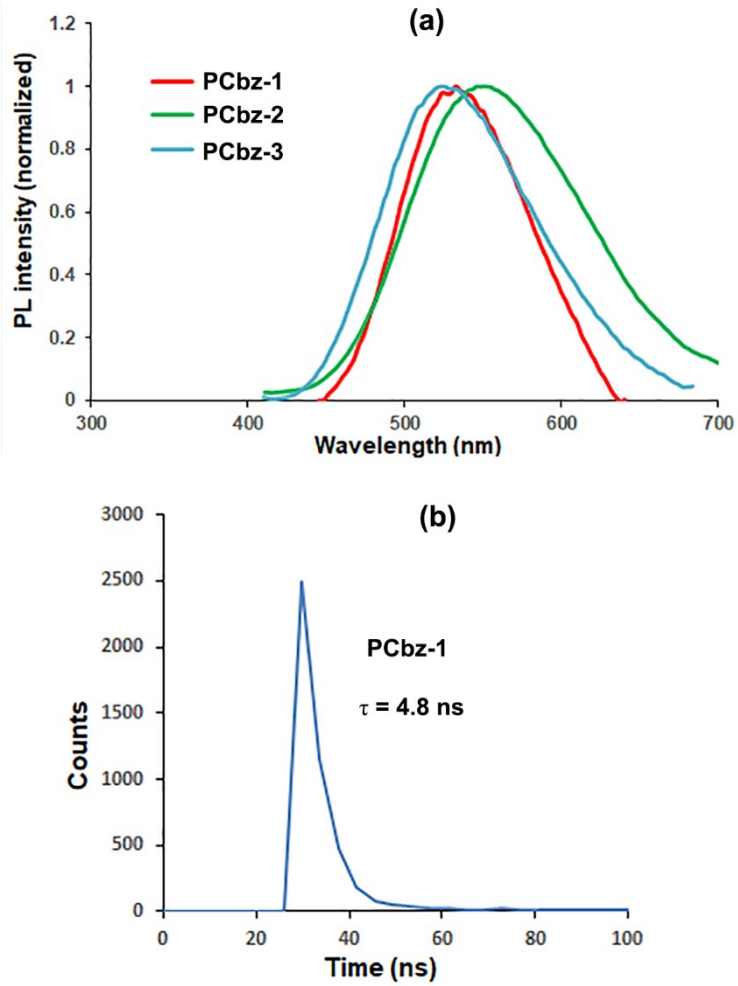

Figure S4. (a) Emission spectra of PCbz-(1–3) in THF. (b). PL decay of PCbz-1.

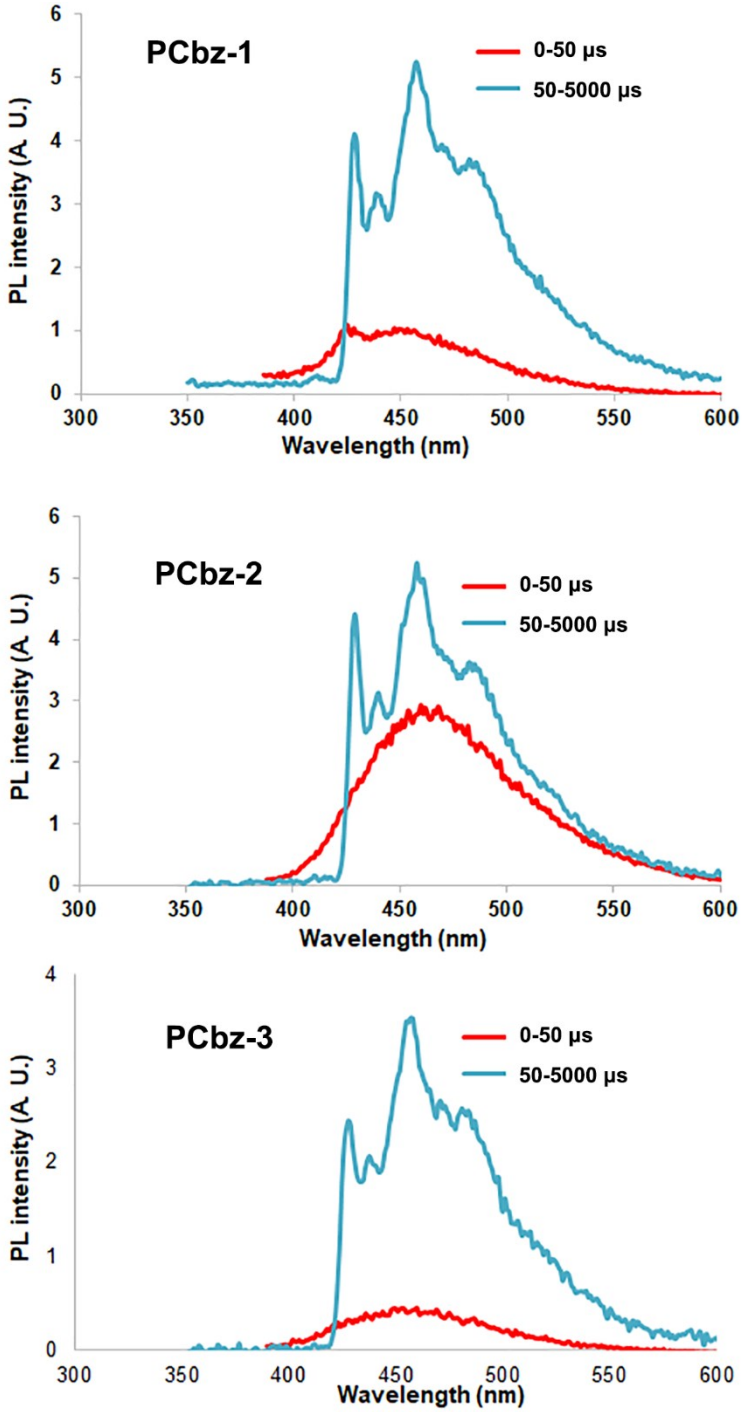

Figure S5. Fluorescence (0-50 µs) and phosphorescence (50-5000 µs) emission bands of the PCbz dyads, measured in 2-MeTHF at 77 K.

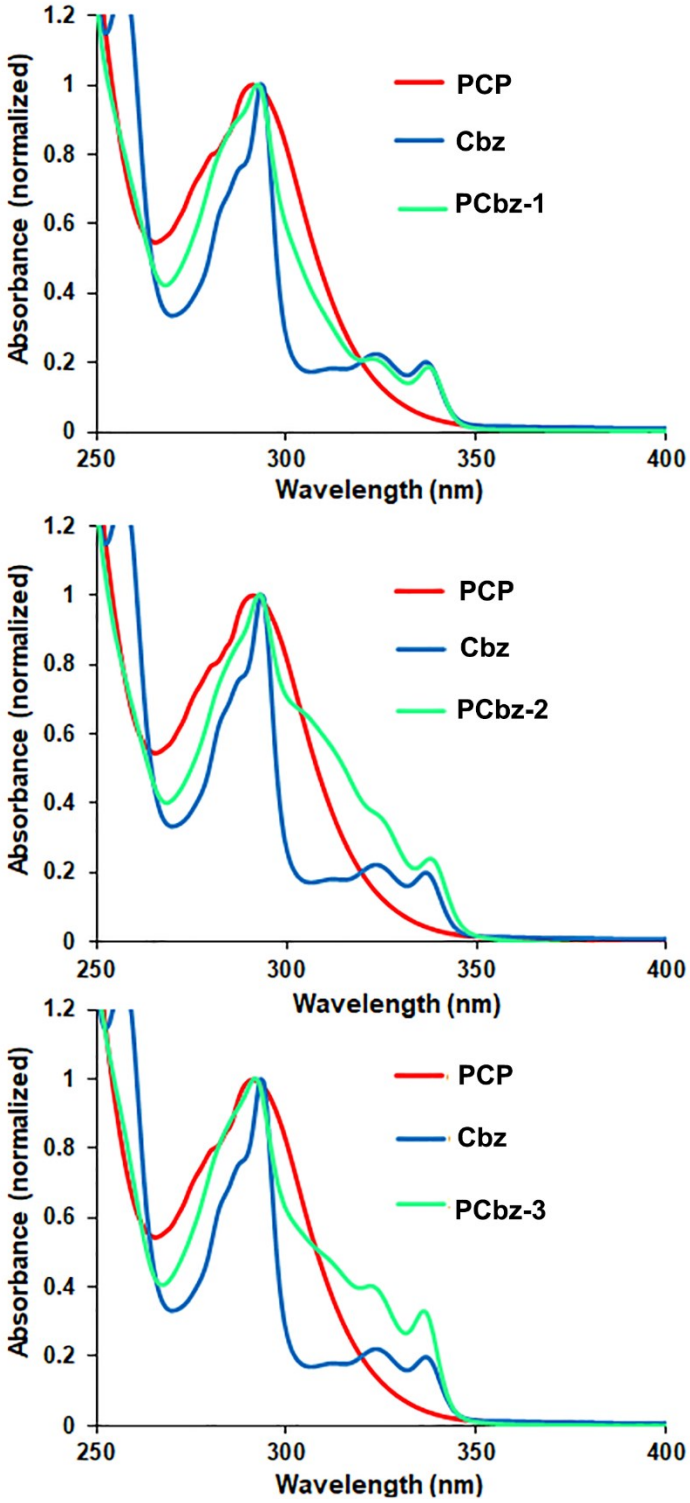

Figure S6. UV-Vis absorption spectra of PCbz dyads in THF solution. Absorption spectra of PCP and Cbz are given for reference.

Table S1 Calculated energies of the lowest singlet and two lowest triplet excited states (MN15/6–31G**, CPCM solvation in THF).

Compound	^{1}CT (S_1) [eV]	$f_{osc., S1}$	^{3}LE$_A$ (T_1) [ev]	^{3}CT (T_2) [eV]	$\Delta E_{S1,T1}$ [eV]	$\Delta E_{S1,T2}$ [eV]
PCbz-1	3.69	0.0012	3.45	3.67	0.24	0.02
PCbz-2	3.75	0.0099	3.44	3.66	0.32	0.10
PCbz-3	3.72	0.0012	3.46	3.71	0.26	0.01

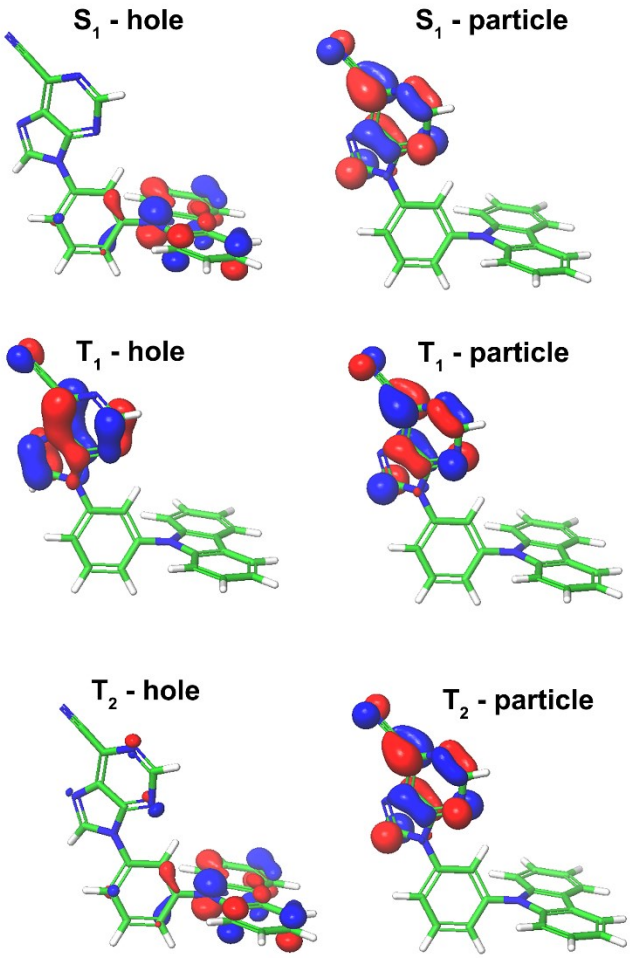

Figure S7. Calculated natural transition orbitals (NTO) for $S_0 \rightarrow S_1$, $S_0 \rightarrow T_1$ and $S_0 \rightarrow T_2$ transitions for PCbz-1 (MN15/6–31G**, CPCM solvation in THF).

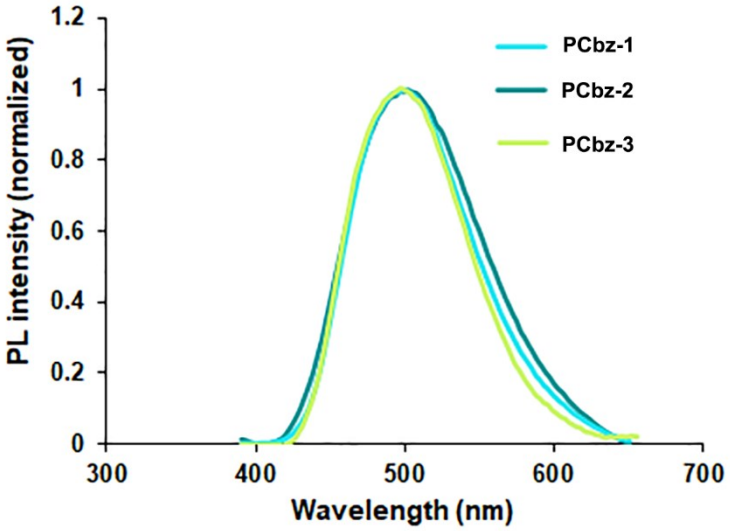

Figure S8. PL spectra of PCbz dyads measured in amorphous neat films.

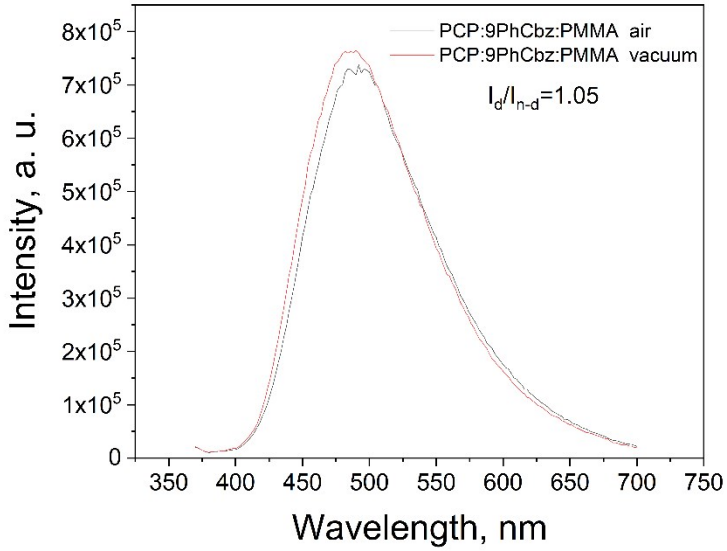

Figure S9. PL intensity of PCP:9-PhCbz exciplex system in air and vacuum, measured in amorphous film.

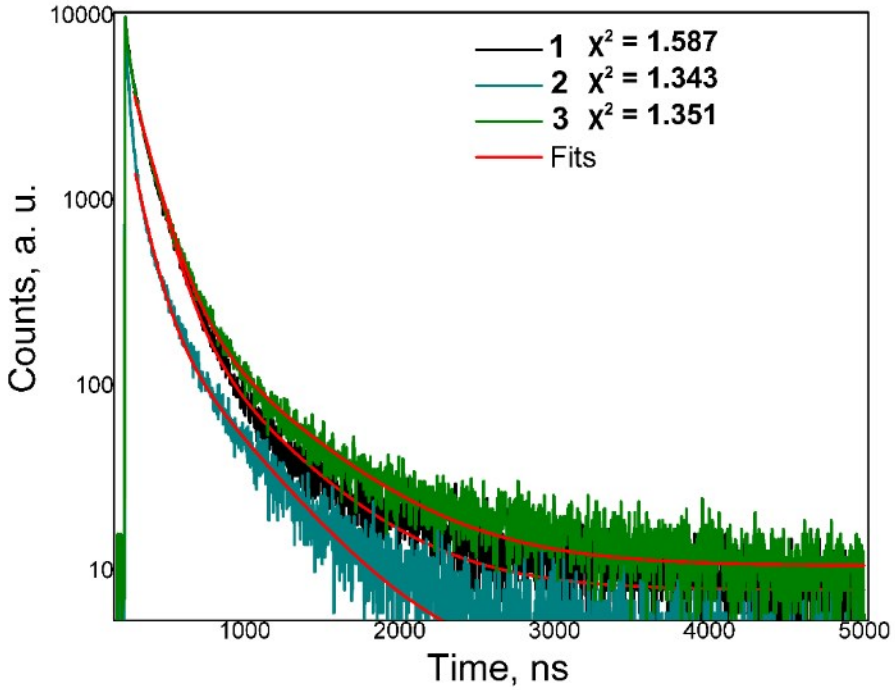

Figure S10. PL decays and fits measured at room temperature in neat films of PCbz(1–3).

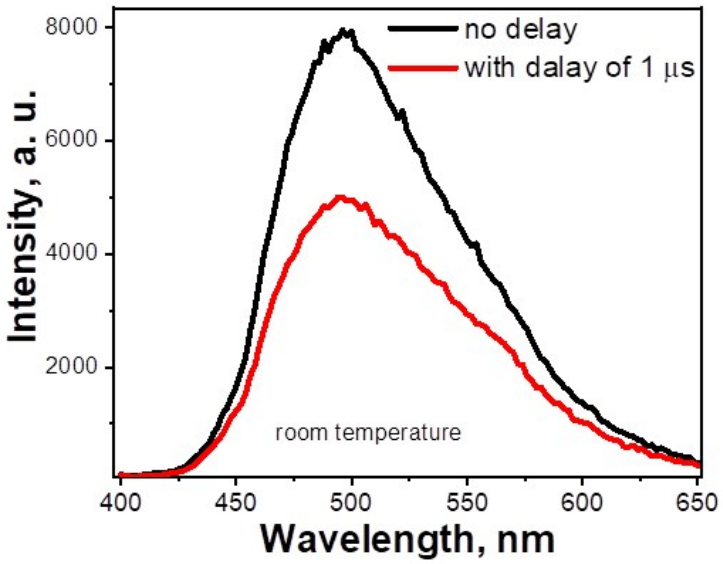

Figure S10. Prompt and delayed PL measured in neat film of PCbz-3.

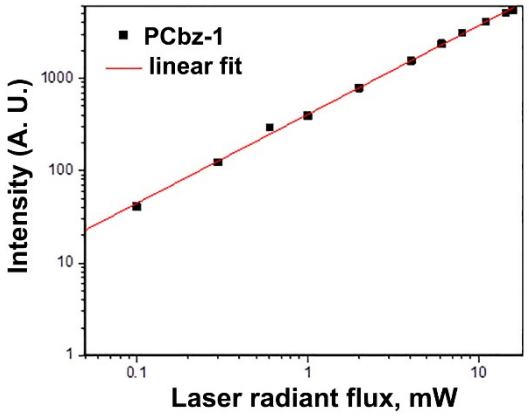

Figure S12. PL intensity and excitation power correlation for PCbz-1 (PL measured at 1–5 μs interval).

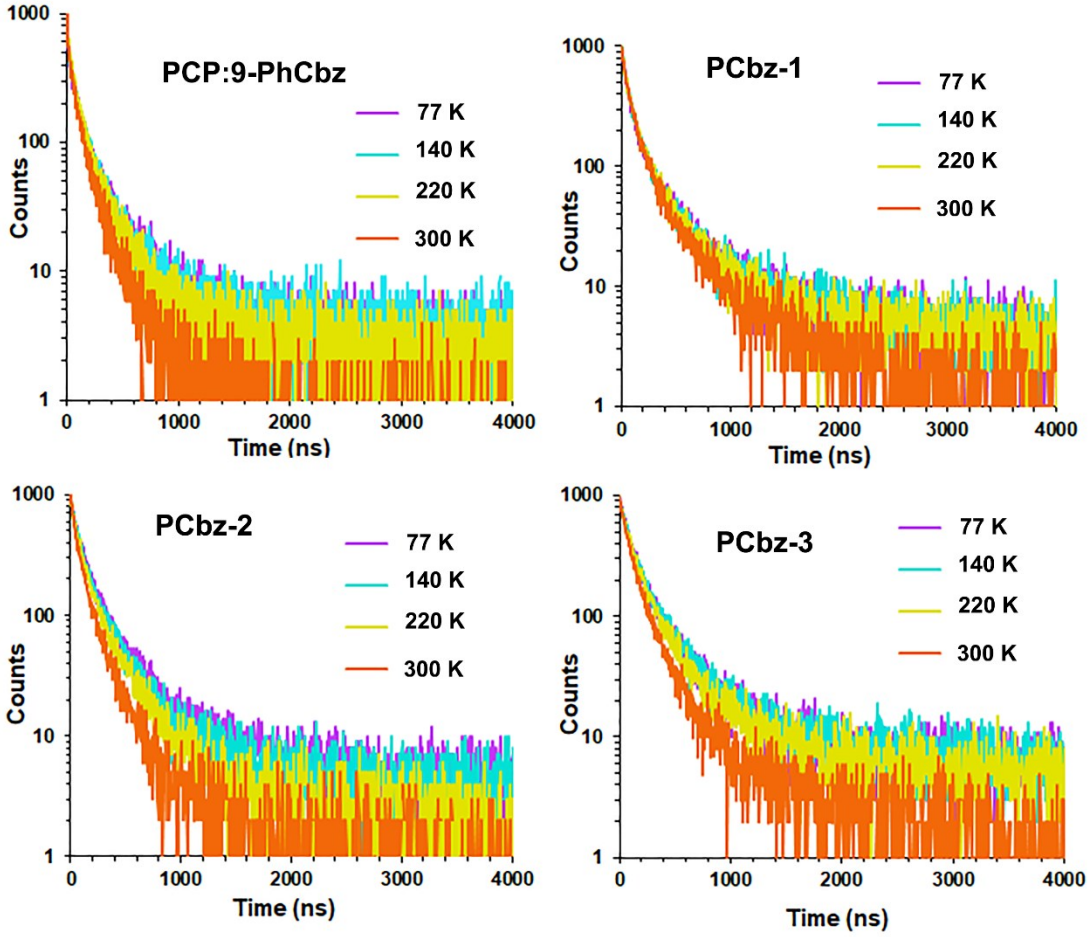

Figure S13. Temperature-dependent PL decay of PCP:9-PhCbz and PCbz(1–3) exciplex systems, measured in neat amorphous films.

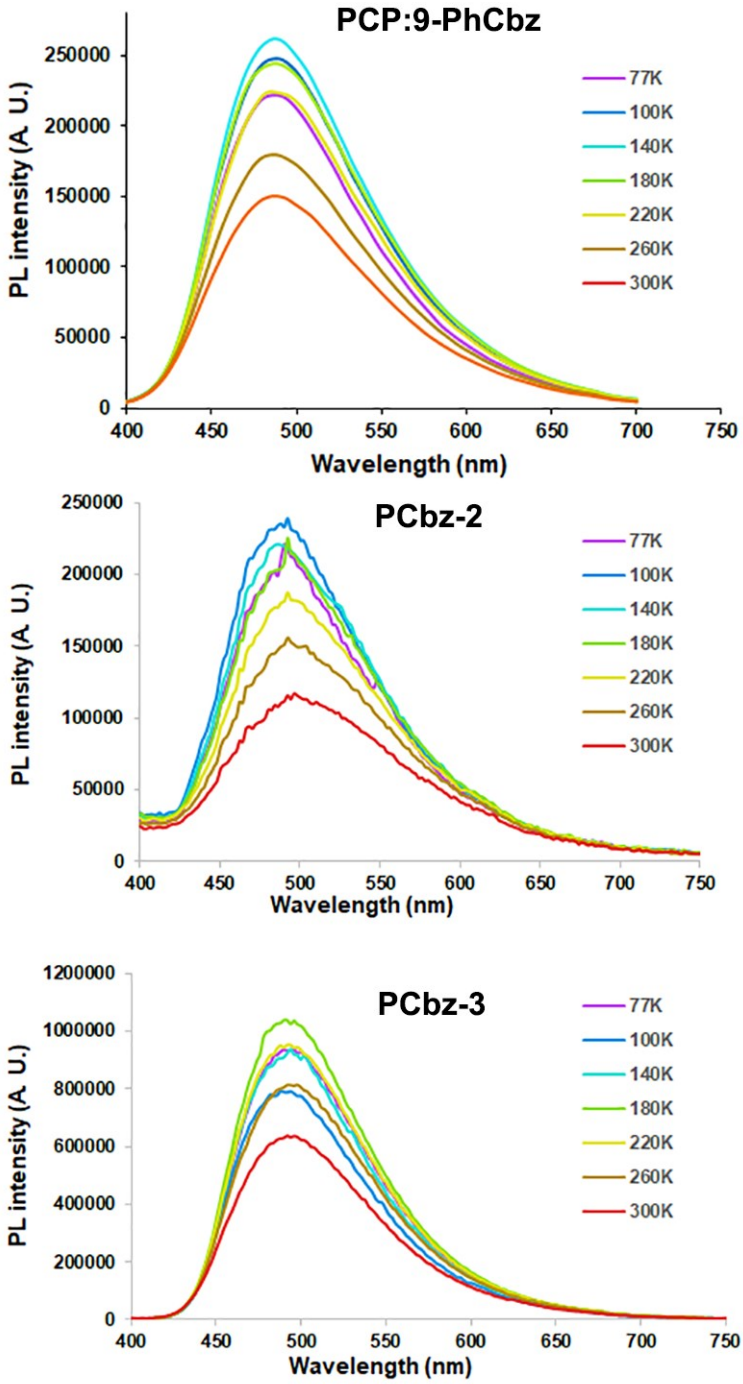

Figure S14. PL intensities versus temperature in neat amorphous films of PCP:9-PhCbz, PCbz-2 and PCbz-3.

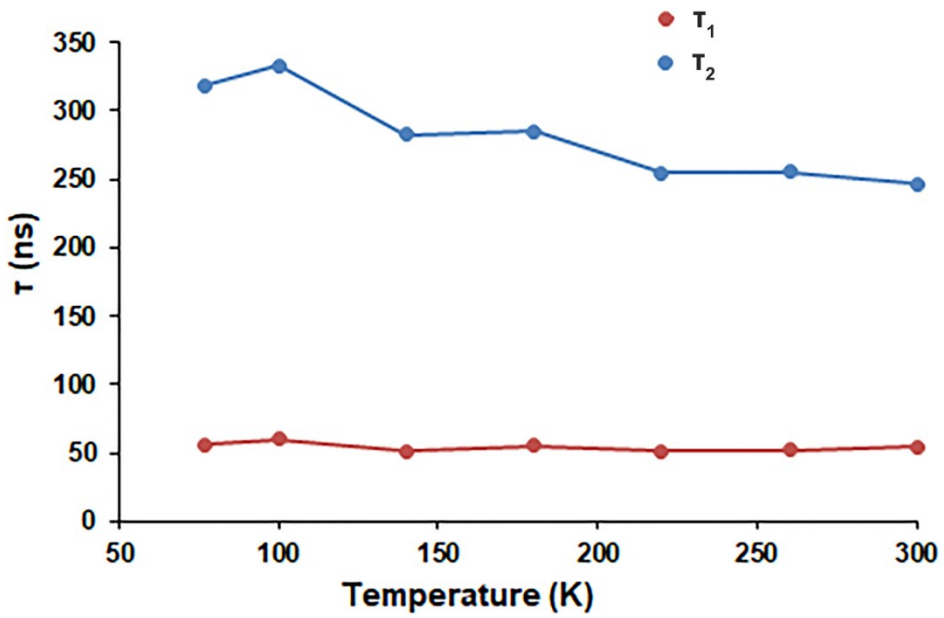

Figure S15. Temperature-dependence of PL decay components τ_1 and τ_2 of PCbz-1, measured in neat film.

Table S2 Photo-physical properties of PCbz–1:PMMA films with different emitter concentration.

Sample	λ_{PL}[a] [nm]	Φ_{PL}	PL lifetime [ns] (contribution of decay components)	E_S[b] [eV]	E_T[c] [eV]	ΔE_{ST}[d] [eV]
1 wt%	468	0.18	6.9 (7%); 63 (41%); 368 (52%)	3.28	2.94	0.34
10 wt%	471	0.23	42 (27%); 143 (73%)	3.09	2.94	0.15
50 wt%	492	0.36	39 (29%); 193 (71%)	2.96	2.94	0.02
Neat film	502	0.41	54 (39%) 246 (61%)	2.82	2.94	-0.12

[a] Emission band maxima. [b] Onset energy of fluorescence at room temperature. [c] Onset energy of PCbz–1 phosphorescence in 2-MeTHF at 77K. [d] $\Delta E_{ST} = E_S - E_T$.

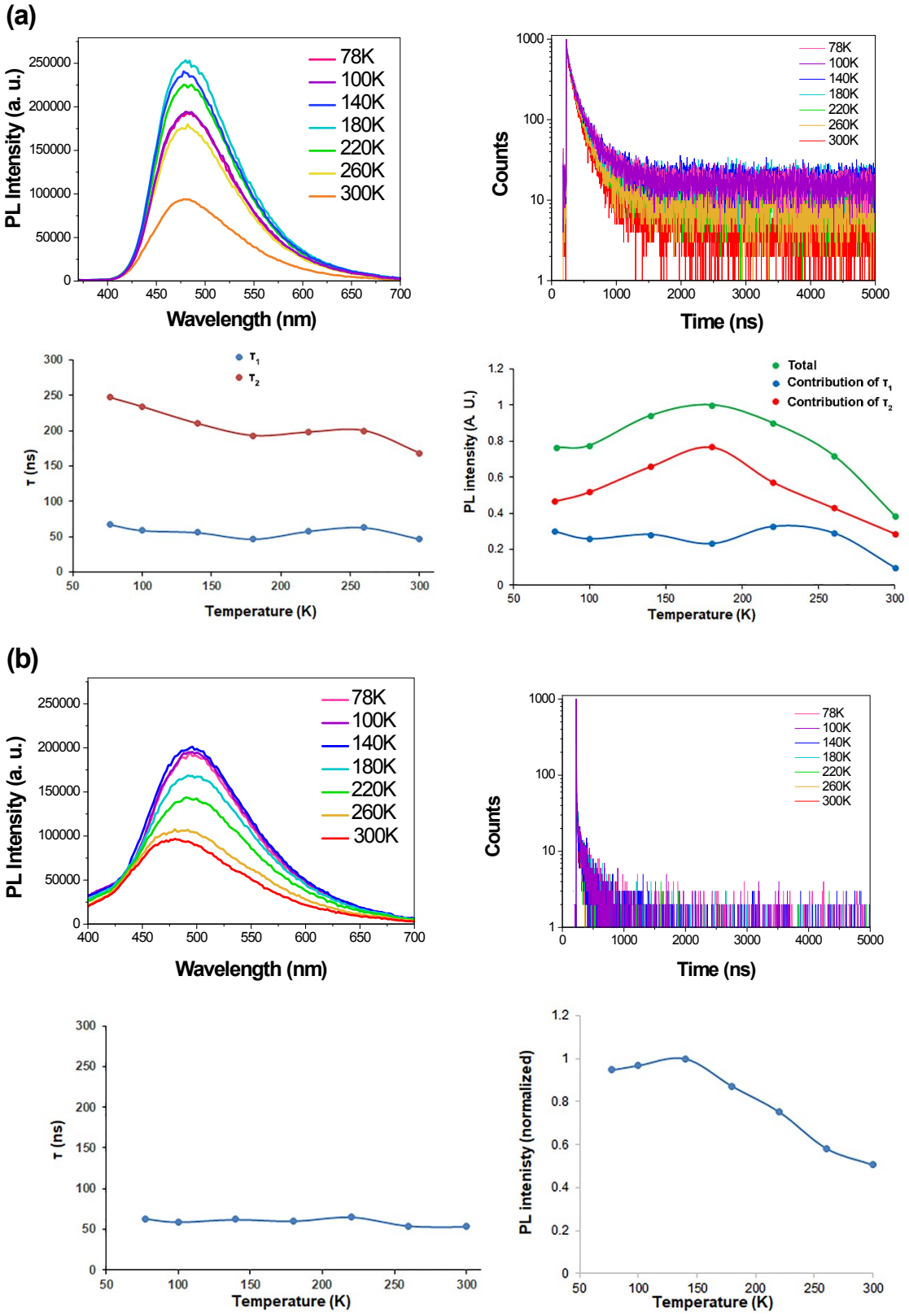

Figure S16. Temperature-dependent measurements of PL bands, PL decays, PL lifetime changes and PL intensity changes for (a) PCP:9-PhCBz (1:2 molar ratio)/PMMA and (b) PCP:9-PhCBz (2:1 molar ratio)/PMMA films. For (b) mixture ^{1}CT PL band partly overlaps with ^1LE_A emission.

Table S3. Hole and electron mobility data for the vacuum-deposited layers of the studied compounds obtained by the TOF measurements.

	Holes			Electrons		
Compound	μ_h (cm^2 V^{-1} s^{-1})*	μ_0 (cm^2 V^{-1} s^{-1})	α (cm V^{-1})$^{1/2}$	μ_e (cm^2 V^{-1} s^{-1})*	μ_0 (cm^2 V^{-1} s^{-1})	α (cm V^{-1})$^{1/2}$
PCbz-1	2.9×10^{-4}	1×10^{-6}	0.0095	4.2×10^{-4}	2.5×10^{-5}	0.0049
PCbz-2	1.2×10^{-4}	2.5×10^{-6}	0.0065	2×10^{-4}	2×10^{-5}	0.0039
PCbz-3	5.1×10^{-4}	1.7×10^{-4}	0.0019	6.5×10^{-4}	2.2×10^{-5}	0.0057

* values recorded at electric field of 3.6×10^5 V/cm. μ_h and μ_e are hole and electron mobilities. μ_0 is zero-field mobility. Field dependence parameter (α) of a Poole–Frenkel type mobility predicted by the relationship $\mu = \mu_0 e^{\alpha E^{1/2}}$. The thickness of the vacuum evaporated layers was in the range from 1.7 to 2.5 μm.

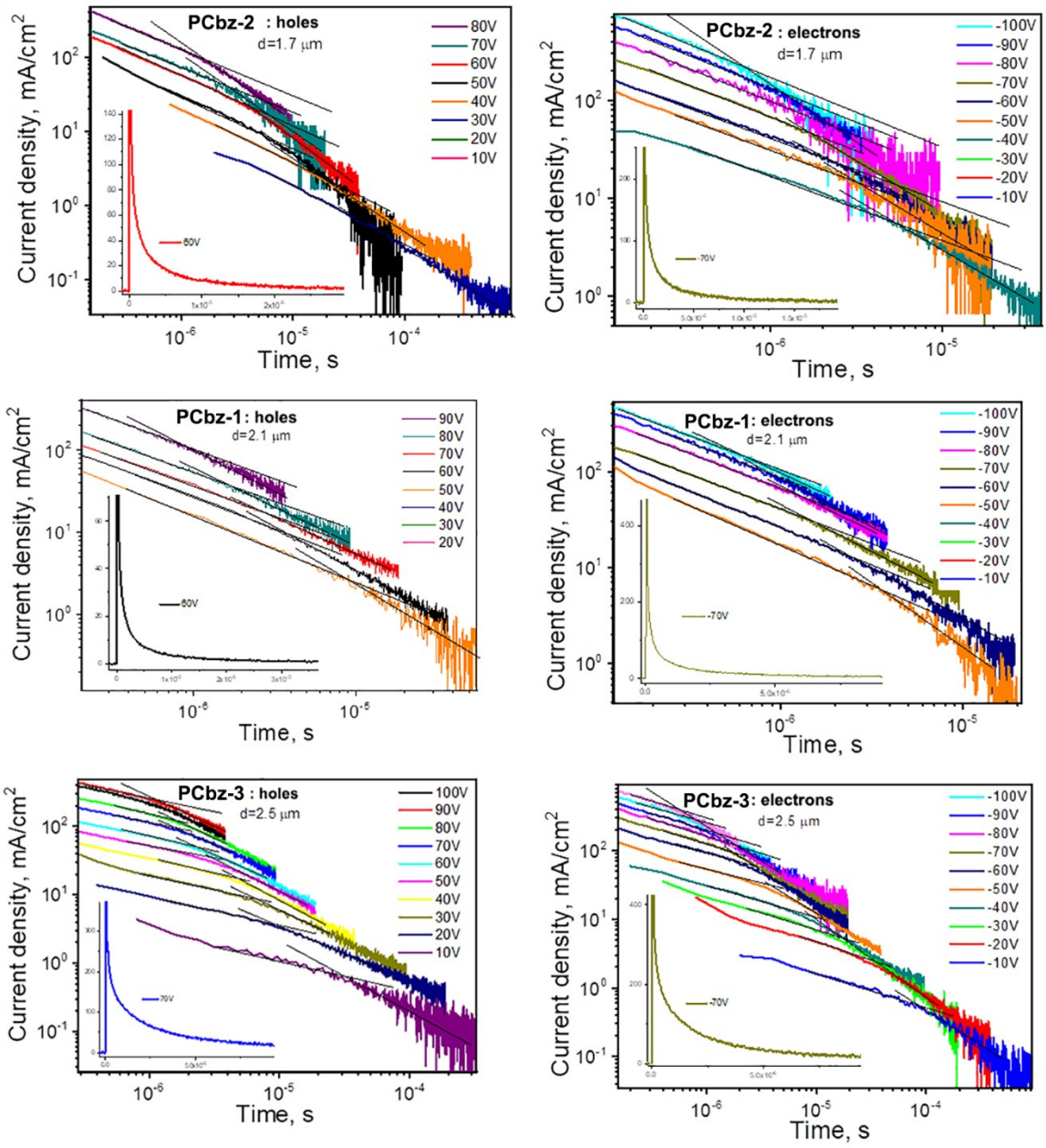

Figure S17. signals for holes and electron in vacuum-deposited films on the studied compounds PCbz(1–3).

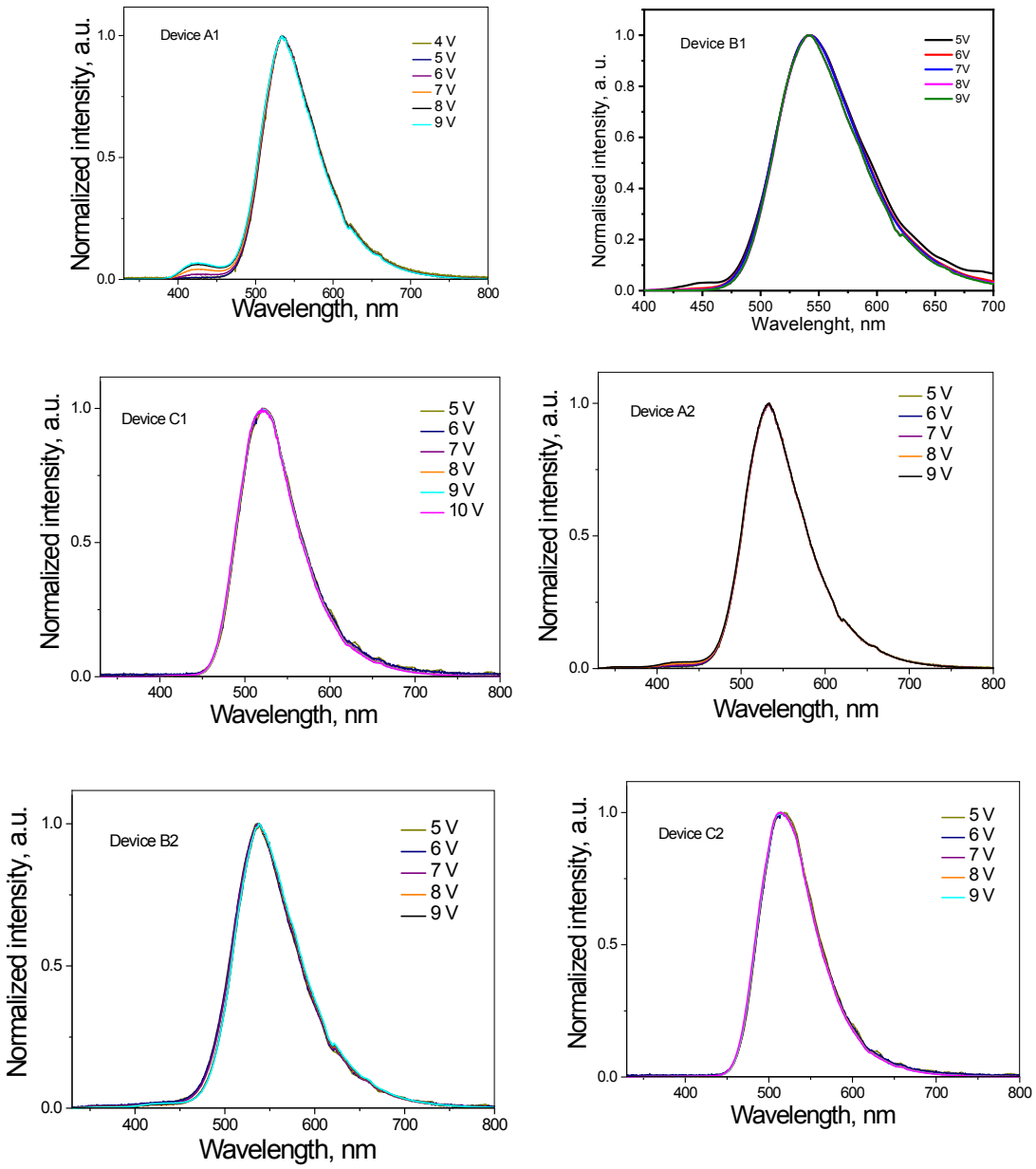

Figure S18. EL spectra of the fabricated devices at different voltages.

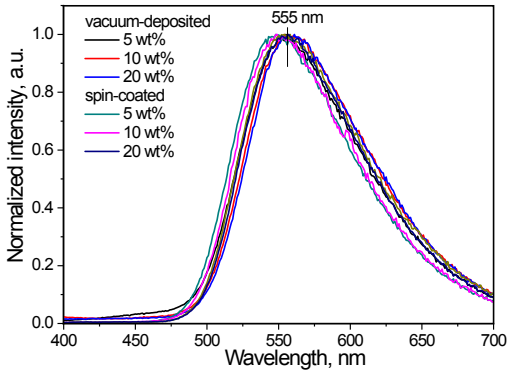

Fig. S19. PL spectra of the doped vacuum deposited and spin-coated layers of DAcIPN:PCbz-3 with the different concentration of DAcIPN.

Experimental section

Optical and electronic measurements

Optical measurements were carried in tetrahydrofuran (THF) solutions with typical material concentrations of 1–4×10^{-5} mol L^{-1}. Deoxygenated solutions were prepared in glovebox under Ar atmosphere, using previously degassed solvent, and filled in sealable quartz cuvettes. Films for optical measurements were prepared using spin-coating technique from THF solution with *a Laurell WS-400B-6NPP/LITE* spincoater on quartz slides, using solutions with material concentration of 5 mg/mL. The UV-Vis spectra were recorded with a *Perkin Elmer Lambda 35* spectrometer. Emission spectra, photoluminescence excitation (PLE) spectra, PL lifetimes in THF, low temperature time-resolved spectra in 2 -MeTHF and Φ_{PL} in films were determined using *QuantaMaster 40* steady state spectrofluorometer (*Photon Technology International, Inc.*) equipped with 6 inch integrating sphere (*LabSphere*). PLE spectra were measured at the maxima of the corresponding emission bands.

PL decays of the studied compounds in neat films were recorded by the *Edinburgh Instruments FLS980* spectrometer exploiting steady-state xenon lamp or pulsed *PicoQuant LDH-D-C-375* laser (wavelength 374 nm) as the excitation source. PL spectra and PL decays in inert atmosphere (N_2) at different temperatures were recorded using the liquid nitrogen cryostat *Optistat DN2*. PL decays were fitted using software from Edinburgh Instruments. Φ_{PL} temperature dependence was determined by integrating emission intensities and calibrating them with Φ_{PL} value measured at room temperature.

Photophysical rate constants for PCbz-1:PMMA (1 wt%) were calculated using conventional equations used for TADF emitters.[1] Experimentally obtained quantum yields and decay lifetimes were used for calculations (Table S2). The following equation were used:

$k_{fluor.} = \frac{\Phi_{prompt}}{\tau_{prompt}}$; $\Phi_{ISC} = \frac{\Phi_{delayed}}{\Phi_{delayed} + \Phi_{prompt}}$, where $\Phi_{delayed}$ was defined as the quantum yield sum of the two delayed emission components; $k_{ISC} = \frac{\Phi_{ISC}}{\tau_{prompt}}$; $k_{RISC} = \frac{1}{\tau_{delayed}} \frac{1}{(1 - \Phi_{ISC})}$; $k_{delayed} = \frac{\Phi_{delayed}}{\tau_{delayed}}$.

Photoemission yield spectroscopy was used to determine ionization potential (IP) and photoconductivity measurements, to determine photoconductivity threshold value (E_{th}). Electron affinity (EA) was then calculated as the difference between IP and E_{th}. IP and E_{th} measurements were carried out on a self-made experimental system, using a procedure described in our previous work.[2]

To estimate hole and electron mobilities of vacuum-deposited layers of the studied compounds, time-of-flight (TOF) method was used. TOF experiments were performed using samples with a structure indium-tin-oxide (ITO) /few μm thick organic layer/aluminium. In TOF setup, a laser (*EKSPLA NL300*, 355 nm wavelength) was used as the excitation source. To check hole and electron transport in the layers at different electric fields, different positive and negative external voltages (U) were applied to the samples employing *6517B* electrometer (*Keithley*). *TDS 3032C* oscilloscope (*Tektronix*) was used to record the photocurrent transients of holes or electrons. Charge mobilities were calculated by the formula $\mu = d^2/(U \times t_{tr})$, where t_{tr} is a transit time, d is the thickness of a layer and U is applied voltage.

Quantum chemical calculations

For PCP density functional theory (DFT) calculations for geometry optimization, time-dependent DFT (TD-DFT) calculations for excited state energies, as well as ISC and fluorescence rate predictions were performed using *ORCA*[3] program package (release 4.2.1). Auxiliary tasks were performed in *Avogadro* program.[4] For ground state geometry optimization CAM–B3LYP[5] functional and Def2–TZVP basis were employed. For excited state geometry optimization (S_1 and T_1) analytical gradient calculations were performed using CAM–B3LYP functional and Def2–TZVP/C basis. RIJCOSX approximation was used for TD-DFT. Excited state energies for all geometries were acquired using CAM–B3LYP/ Def2–TZVP theory level. ISC and fluorescence rates were obtained using excited state dynamics (ESD) module. Previously obtained ground state and S_1 state geometries and the corresponding Hessians (from analytical frequency calculations) were used as the input for the fluorescence rate calculations. For ISC the input consisted of S_1 and T_1 geometries and the corresponding Hessians. The contribution of Herzberg-Teller (HT) effect was accounted for ISC. The overall ISC rate was obtained as the sum of three triplet spin-sublevel (-1, 0, 1) contributions: $1.16 \cdot 10^8$ s^{-1} (0); $1.62 \cdot 10^8$ s^{-1} (-1) and $1.62 \cdot 10^8$ s^{-1} (1).

Calculations for PCbz(1–3) were performed using Schrödinger (release 2020–2) Jaguar[6] software package. Geometry optimization and TD-DFT calculations employed MN15[7] functional and 6–31G** basis. Conductor-like polarizable continuum model CPCM model for THF was used.

OLED preparation and characterization

To fabricate devices, materials hexaazatriphenylenehexacarbonitrile (HATCN), N,N′-di(1-naphthyl)-N,N′-diphenyl-(1,1′-biphenyl)-4,4′-diamine (NPB), 1,3-bis(9-carbazolyl)benzene (mCP), diphenyl-4-triphenylsilyl-phenylphosphineoxide (TSPO1) and 2,2',2''-(1,3,5-benzinetriyl)-tris(1-phenyl-1-H-benzimi-dazole) (TPBi) were purchased from Sigma Aldrich or Lumtec and used as received.

Electroluminescent devices were fabricated by vacuum deposition of organic and metal layers onto pre-cleaned ITO coated glass substrates under vacuum higher than 2×10^{-6} mBar. ITO-coated glass substrates with a sheet resistance of 15 Ω/sq were pre-patterned getting seven independent devices with area 6 mm^2. Density-voltage and luminance-voltage characteristics were recorded utilizing certificated photodiode PH100-Si-HA-D0 together with the PC-Based Power and Energy Monitor 11S-LINK (from STANDA) and Keithley 2400C source meter. Electroluminescence (EL) spectra were taken by the Avantes AvaSpec-2048XL spectrometer. Device efficiencies were calculated using the luminance, current density, and EL spectra.

Synthesis and characterization

The solvents used in the reactions were dried with standard drying agents and freshly distilled prior to use. Commercially available reagents were used as received. [4-(9*H*-Carbazol-9-yl)phenyl]boronic acid and [3-(9*H*-carbazol-9-yl)phenyl]boronic acid were purchased from *Fluorochem Ltd*, while [3,5-di(9*H*-carbazol-9-yl)phenyl]boronic acid[6] and 6-cyano-9-phenylpurine (PCP)[7] was prepared according to literature. All reactions were followed by: TLC on *E. Merck Kieselgel 60 F254*, with detection by UV light; HPLC analysis; NMR analysis. Column chromatography was performed on silica gel (60 Å, 40–63 μm, *ROCC*). Melting points were recorded with a *Fisher Digital Melting Point Analyzer Model 355* apparatus. IR spectra were recorded in hexachlorobutadiene (4000–2000 cm^{-1}) and paraffin oil (2000–450 cm^{-1}) with *FTIR Perkin– Elmer Spectrum 100* spectrometer. Crystallographic diffraction data were collected with a *NoniusKappa CCD* diffractometer (Mo-Kα, λ = 0.71073 Å) equipped with a low temperature *Oxford Cryosystems Cryostream Plus* device. Crystallographic data for PCbz-2 are deposited at the Cambridge Crystallographic Data Centre as Supplementary Publication Number CCDC 1988182.

^{1}H and ^{13}C NMR spectra were recorded with a *Bruker 500 MHz* spectrometers in $CDCl_3$. Chemical shifts (δ) are reported in ppm and coupling constants (*J*) in Hz. Residual solvent (^{1}H) or solvent (^{13}C) peaks were used as internal reference ($CDCl_3$: δ = 7.26 ppm for ^{1}H NMR; $CDCl_3$ δ = 77.16 ppm for ^{13}C NMR). Multiplicities are indicated as follows: s (singlet), d (doublet), t (triplet), q (quartet), m (multiplet). The non-trivial peak assignments were confirmed with 2D ^{1}H–^{1}H COSY/HMBC and/or 2D HSQC ^{1}H-^{13}C NMR for representative products within each compound class. HPLC analysis was performed using *Agilent Technologies 1200 Series* system equipped with *XBridge C18* column, 4.6×150 mm, particle size 3.5 μm, with flow rate of 1 mL/min, using 0.1% TFA/H_2O and MeCN for mobile phase. Wavelength of detection was 260 nm. Eluent A – 0.1% TFA aqueous solution with 5% v/v MeCN, eluent B – MeCN. Eluent E_1: gradient 30–95% B 5 min, 95% B 5 min, 95–30% B 2 min. Eluent E_2: gradient 80–95% B 5 min, 95% B 5 min, 95–80% B 2 min. LC/MS was recorded with *Waters Acquity UPLC* system equipped with *Acquilty UPLC BEH* C18 1.7 μm, 2.1×50 mm; using 0.1% TFA/H_2O and MeCN for mobile phase. HRMS analyses were performed on *Agilent 1290 Infinity series UPLC* system equipped with column Extend C18 RRHD 2.1×50 mm, 1.8 μm connected to *Agilent 6230 TOF* LC/MS masspectrometer. Oil bath with controlled temperature was used for all reactions that were carried out at elevated temperatures.

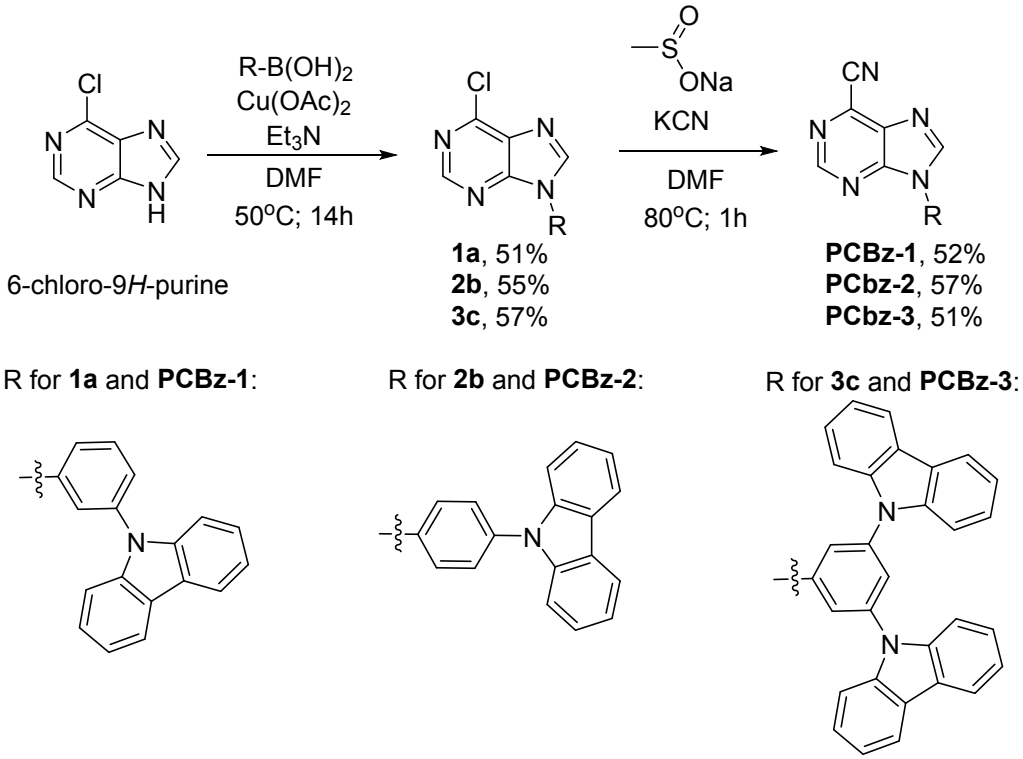

Scheme S1. Synthesis of purinylcarbazoles **PCbz-1, PCbz-2, PCbz-3**

9-[3-(6-Chloro-9*H*-purin-9-yl)phenyl]-9*H*-carbazole (1a)

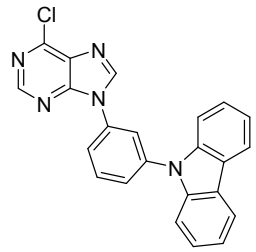

General method A for Chan-Lam coupling: To a solution of 6-chloro-9*H*-purine (540 mg, 3.48 mmol, 1.0 eq.), [3-(9*H*-carbazol-9-yl)phenyl]boronic acid (**a**) (2.0 g, 6.96 mmol, 2.0 eq.) and anhydrous $Cu(OAc)_2$ (634 mg, 3.48 mmol, 1.0 eq.) in dry DMF (50 mL) 4Å molecular sieves (4.0 g) and Et_3N (1.44 mL, ρ = 0.73 g/cm^3, 10.46 mmol, 3.0 eq.) were added and the reaction mixture was stirred for 14 h at 50 °C under a reflux condenser. Then it was centrifuged, the solution was subsequently filtered through celite and washed with DMF (2×5 mL). Filtrate was evaporated and dried in vacuum overnight. Silica gel column chromatography (DCM/MeCN, gradient 0% → 4%) provided product **1a** (yield: 703 mg, 51%) as a colorless solid. R_f = 0.36 (DCM/MeCN = 20:1). HPLC: t_R = 7.14 min, eluent E_1. IR (KBr) ν (cm^{-1}): 3123, 3040, 1611, 1591, 1498, 1453, 1346, 1225, 1208. ^{1}H-NMR (500 MHz, $CDCl_3$) δ (ppm): 8.85 (s, 1H, H-C(2)), 8.50 (s, 1H, H-C(8)), 8.17 (d, 2H, ^3J = 7.6 Hz, 2×H-C(Ar)), 8.08 (t, 1H, ^4J = 2.0 Hz, H-C(Ar)), 7.86 (t, 1H, ^3J = 8.0 Hz, H-C(Ar)), 7.81 (ddd, 1H, ^3J = 8.0 Hz, ^4J = 2.0 Hz, ^4J = 1.4 Hz, H-C(Ar)), 7.77 (ddd, 1H, ^3J = 8.0 Hz, ^4J = 2.0 Hz, ^4J = 1.4 Hz, H-C(Ar)), 7.57 (d, 2H, ^3J = 7.8 Hz, 2×H-C(Ar)), 7.57 (t, 2H, ^3J = 7.8 Hz, 2×H-C(Ar)),

7.34 (t, 2H, ^{3}J = 7.6 Hz, 2×H-C(Ar)). ^{13}C-NMR (126 MHz, $CDCl_3$) δ (ppm): 153.0, 152.1, 151.6, 143.8, 140.5, 139.8, 135.5, 132.4, 131.6, 127.2, 126.4, 123.9, 122.0, 121.7, 120.8, 120.7, 109.7. HRMS (ESI) m/z: $[M+H]^+$ Calcd for $C_{23}H_{15}ClN_5$ 396.1010; Found 396.1025.

^{1}H-NMR (500 MHz, $CDCl_3$) spectrum of compound 1a:

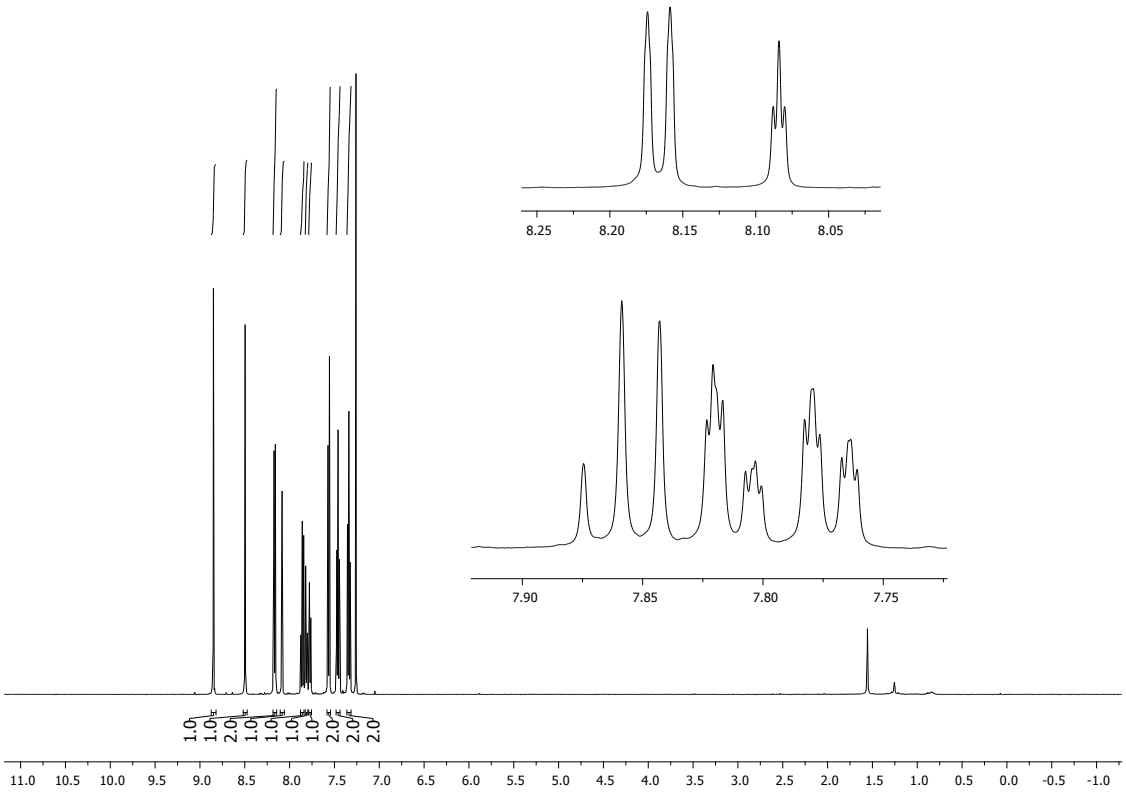

^{13}C-NMR (126 MHz, $CDCl_3$) spectrum of compound 1a:

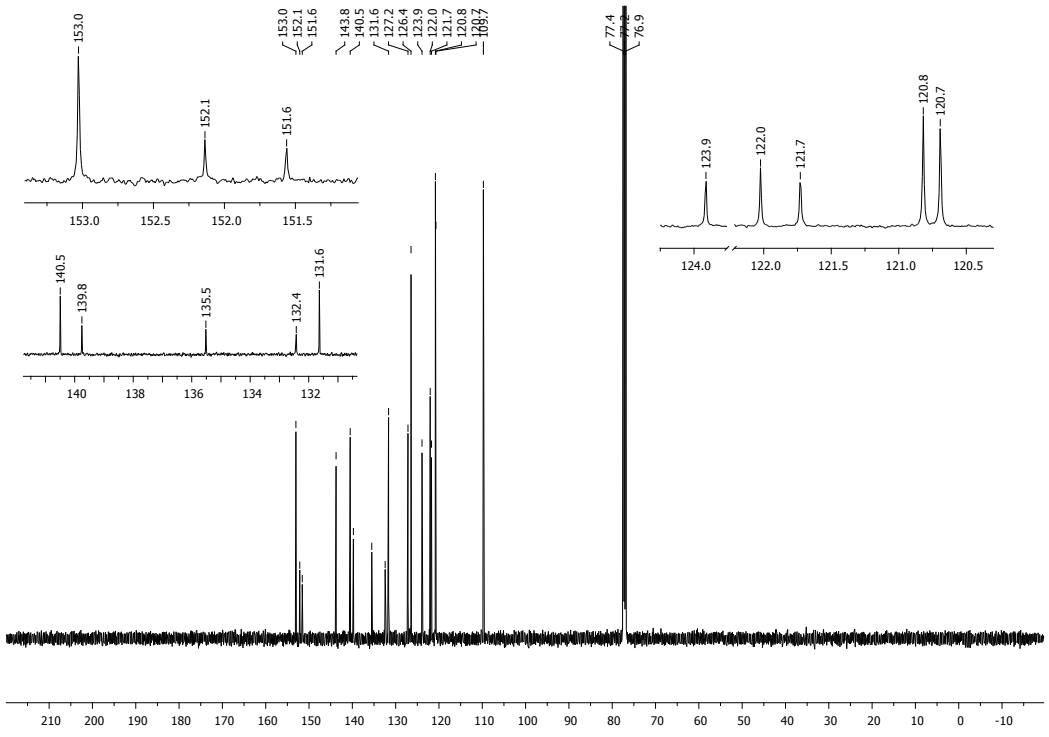

9-[4-(6-Chloro-9*H*-purin-9-yl)phenyl]-9*H*-carbazole (2b)

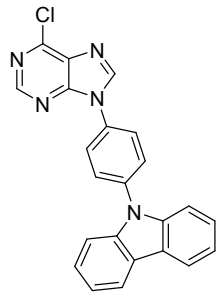

Syntesized according to general method A: 6-chloro-9*H*-purine (270 mg, 1.74 mmol, 1.0 eq.), [4-(9*H*-carbazol-9-yl)phenyl]boronic acid (**b**) (1.0 g, 3.48 mmol, 2.0 eq.), anhydrous $Cu(OAc)_2$ (317 mg, 1.74 mmol, 1.0 eq.), 4Å molecular sieves (4.0 g), Et_3N (0.72 mL, ρ = 0.73 g/cm^3, 5.22 mmol, 3.0 eq.), dry DMF (30 mL), 14 h, 50 °C. Silica gel column chromatography (DCM/MeCN, gradient 0% → 5%) provided product **2b** (yield: 378 mg, 55%) as a colorless solid. R_f = 0.33 (DCM/MeCN = 20:1). HPLC: t_R = 7.04 min, eluent E_1. IR (KBr) ν (cm^{-1}): 3052, 1581, 1556, 1520, 1452, 1337, 1218, 1197. ^{1}H-NMR (500 MHz, $CDCl_3$) δ (ppm): 8.89 (s, 1H, H-C(2)), 8.52 (s, 1H, H-C(8)), 8.17 (d, 2H, ^3J = 7.4 Hz, 2×H-C(Ar)), 7.99 (d, 2H, ^3J = 8.6 Hz, 2×H-C(Ar)), 7.85 (d, 2H, ^3J = 8.6 Hz, 2×H-C(Ar)), 7.49 (t, 2H, ^3J = 7.9 Hz, 2×H-C(Ar)), 7.45 (d, 2H, ^3J = 7.9 Hz, 2×H-C(Ar)), 7.34 (t, 2H, ^3J = 7.4 Hz, 2×H-C(Ar)). ^{13}C-NMR (126 MHz, $CDCl_3$) δ (ppm): 153.0, 152.2, 151.6, 144.0, 140.6, 138.6, 132.7, 132.4, 128.7, 126.4, 125.1, 123.8, 120.7 (2C), 109.7. HRMS (ESI) m/z: $[M+H]^+$ Calcd for $C_{23}H_{15}ClN_5$ 396.1010; Found 396.1006.

^{1}H-NMR (500 MHz, $CDCl_3$) spectrum of compound 2b:

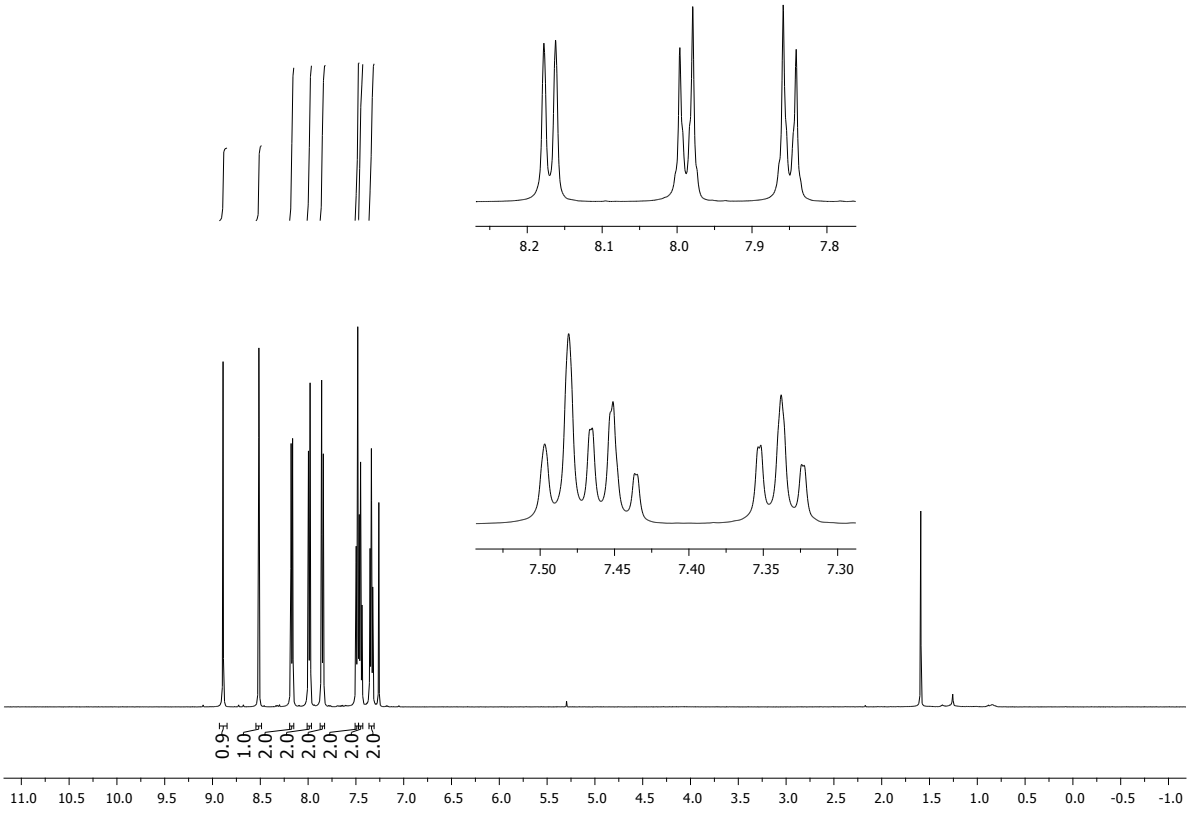

^{13}C-NMR (126 MHz, $CDCl_3$) spectrum of compound 2b:

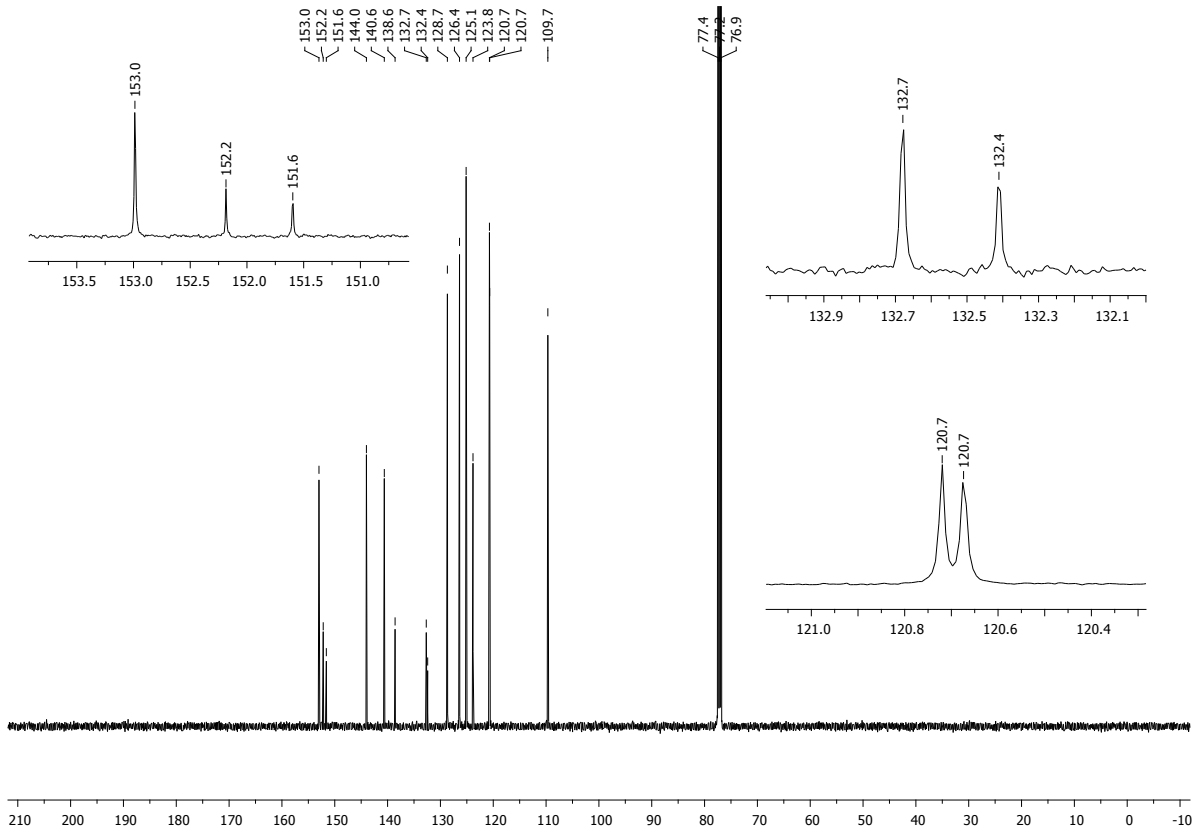

9,9'-[5-(6-Chloro-9*H*-purin-9-yl)-1,3-phenylene]bis(9*H*-carbazole) (3c)

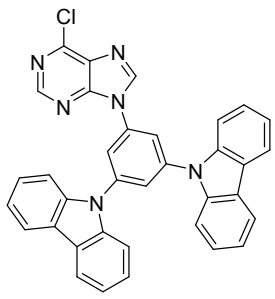

Synthesized according to general method A: 6-chloro-9*H*-purine (160 mg, 1.03 mmol, 1.0 eq.), [3,5-di(9*H*-carbazol-9-yl)phenyl]boronic acid (**c**) (927 mg, 2.06 mmol, 2.0 eq.), anhydrous $Cu(OAc)_2$ (187 mg, 1.03 mmol, 1.0 eq.), 4Å molecular sieves (2.0 g), Et_3N (0.43 mL, $\rho = 0.73$ g/cm^3, 3.08 mmol, 3.0 eq.), dry DMF (20 mL), 14 h, 50 °C. Silica gel column chromatography (DCM/MeCN, gradient 0% → 2%) provided product **3c** (yield: 326 mg, 57%) as a colorless solid. R_f = 0.41 (DCM/MeCN = 20/1). HPLC: t_R = 7.40 min, eluent E_2. IR (KBr) ν (cm^{-1}): 3051, 1602, 1579, 1464, 1440, 1334, 1225, 919. ^{1}H-NMR (500 MHz, $CDCl_3$) δ (ppm): 8.89 (s, 1H, H-C(2)), 8.56 (s, 1H, H-C(8)), 8.22–8.14 (m, 6H, 6×H-C(Ar)), 8.02 (t, 1H, ^4J = 1.7 Hz, H-C(Ar)), 7.69 (d, 4H, ^3J = 8.3 Hz, 4×H-C(Ar)), 7.50 (t, 4H, ^3J = 7.6 Hz, 4×H-C(Ar)), 7.36 (t, 4H, ^3J = 7.6 Hz, 4×H-C(Ar)). ^{13}C-NMR (126 MHz, $CDCl_3$) δ (ppm): 153.2, 152.4, 151.5, 143.3, 141.2, 140.3, 136.7, 132.5, 126.7, 124.5, 124.1, 121.2, 120.8, 119.6, 109.7. HRMS (ESI) m/z: $[M+H]^+$ Calcd for $C_{35}H_{22}ClN_6$ 561.1589; Found 561.1576.

^{1}H-NMR (500 MHz, $CDCl_3$) spectrum of compound 3c:

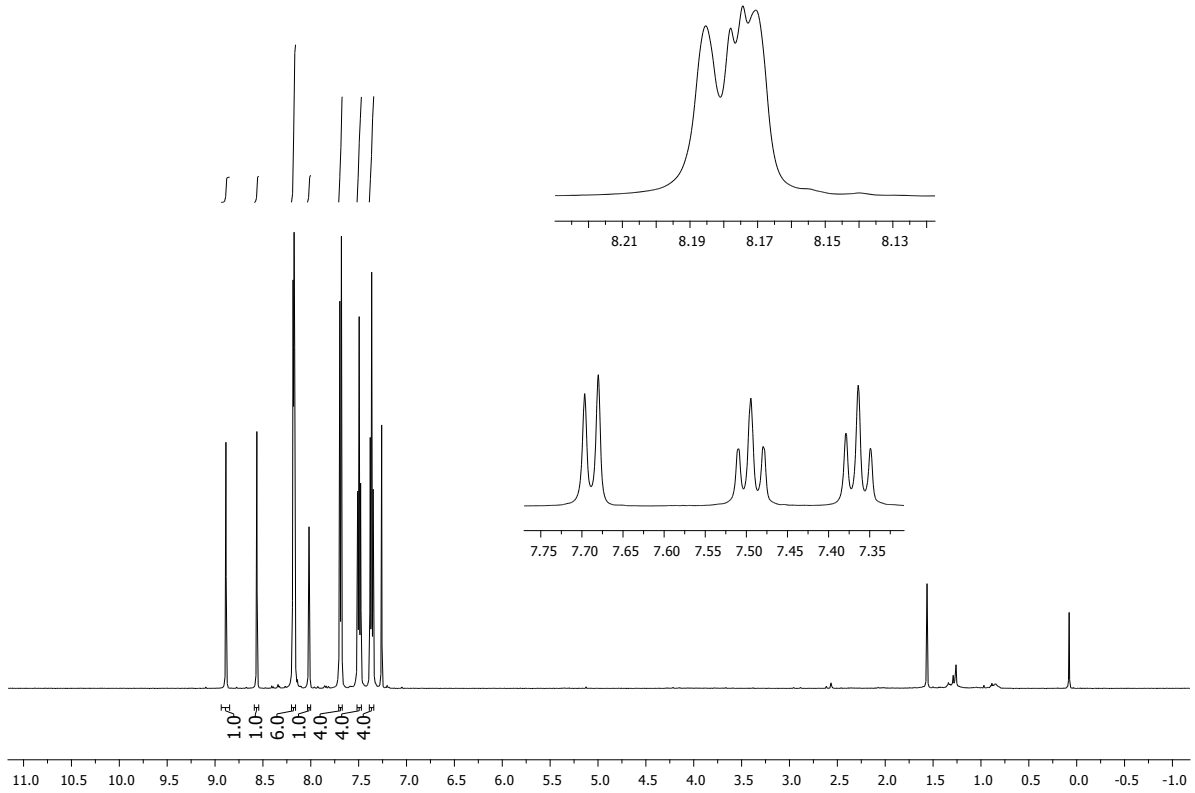

^{13}C-NMR (126 MHz, $CDCl_3$) spectrum of compound 3c:

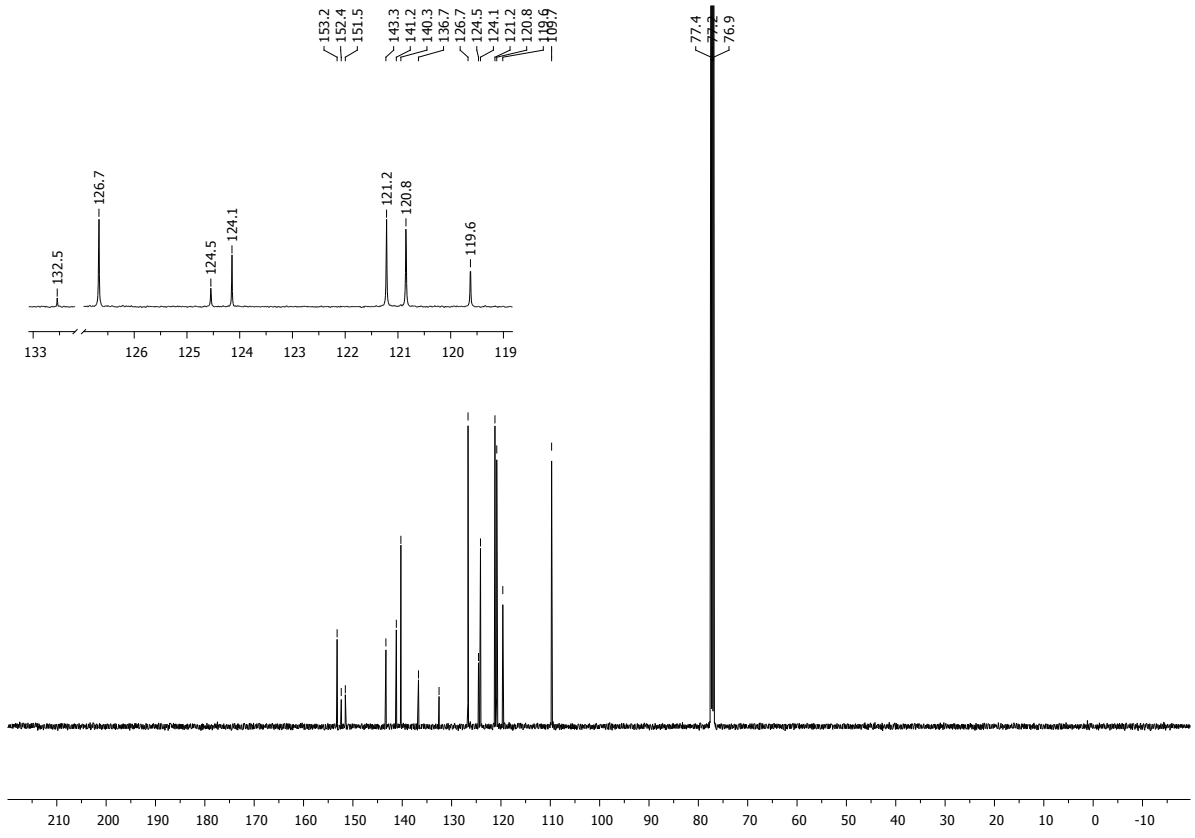

9-(3-(9*H*-Carbazol-9-yl)phenyl)-9*H*-purine-6-carbonitrile (PCBz-1)

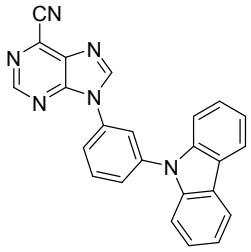

General method B for sulfinate mediated cyanide introduction: To a solution of compound **1a** (250 mg, 0.63 mmol, 1.0 eq.) and sodium methanesulfinate salt (64 mg, 0.63 mmol, 1.0 eq.) in dry DMF (8 mL) KCN (82 mg, 1.26 mmol, 2.0 eq.) was added and the reaction mixture was stirred for 1 h at 80 °C. Then it was evaporated and dried in vacuum overnight. Silica gel column chromatography (DCM/MeCN, gradient 0% → 4%) provided product **PCbz-1** (yield: 127 mg, 52%) as a pale yellow solid. R_f = 0.64 (DCM/MeCN = 20:1). HPLC: t_R = 7.21 min, eluent E_1. IR (KBr) ν (cm^{-1}): 3052, 2924, 2243, 1591, 1509, 1463, 1450, 1335, 1225. ^{1}H-NMR (500 MHz, $CDCl_3$) δ (ppm): 9.16 (s, 1H, H-C(2)), 8.65 (s, 1H, H-C(8)), 8.17 (d, 2H, ^3J = 7.6 Hz, 2×H-C(Ar)), 8.09 (s, 1H, H-C(Ar)), 7.88 (t, 1H, ^3J = 8.0 Hz, H-C(Ar)), 7.81 (d, 2H, ^3J = 8.0 Hz, 2×H-C(Ar)), 7.56 (d, 2H, ^3J = 7.9 Hz, 2×H-C(Ar)), 7.46 (t, 2H, ^3J = 7.9 Hz, 2×H-C(Ar)), 7.34 (t, 2H, ^3J = 7.6 Hz, 2×H-C(Ar)). ^{13}C-NMR (126 MHz, $CDCl_3$) δ (ppm): 153.7, 152.6, 146.5, 140.5, 139.9, 135.7, 134.9, 132.1, 131.8, 127.5, 126.5, 123.9, 122.1, 121.7, 120.9, 120.7, 113.5, 109.7. HRMS (ESI) m/z: $[M+H]^+$ Calcd for $C_{24}H_{15}N_6$ 387.1353; Found 387.1338.

^{1}H-NMR (500 MHz, $CDCl_3$) spectrum of compound PCbz-1:

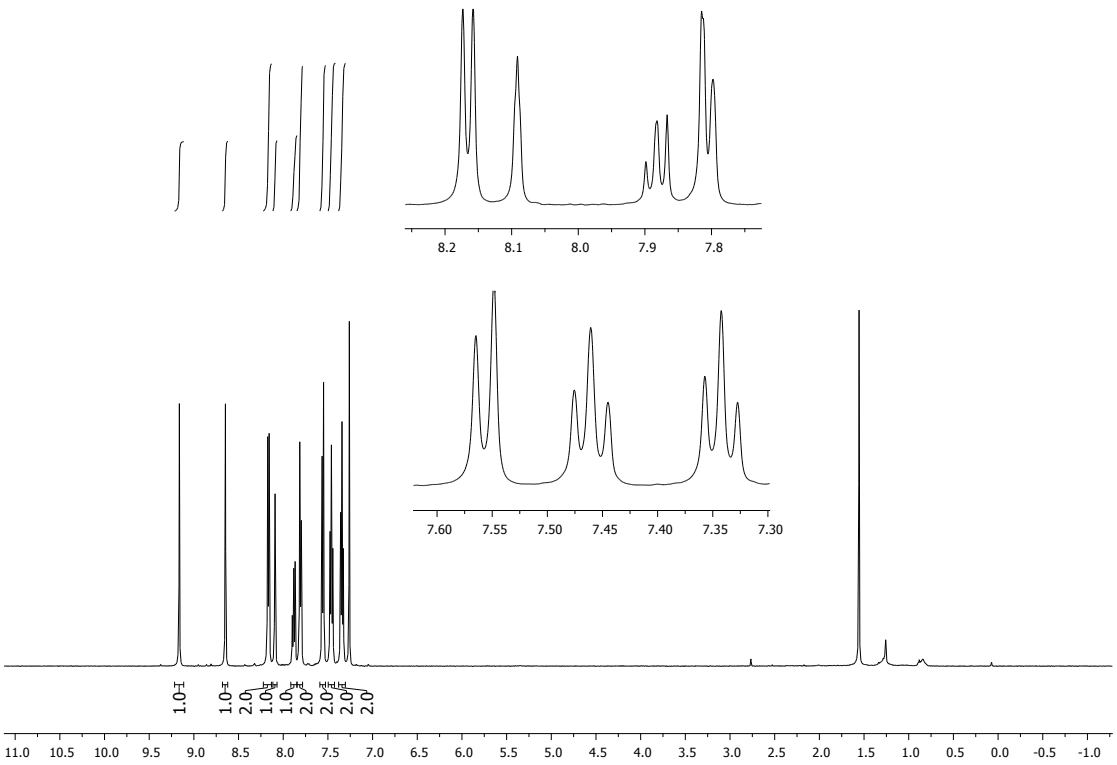

^{13}C-NMR (126 MHz, $CDCl_3$) spectrum of compound PCbz-1:

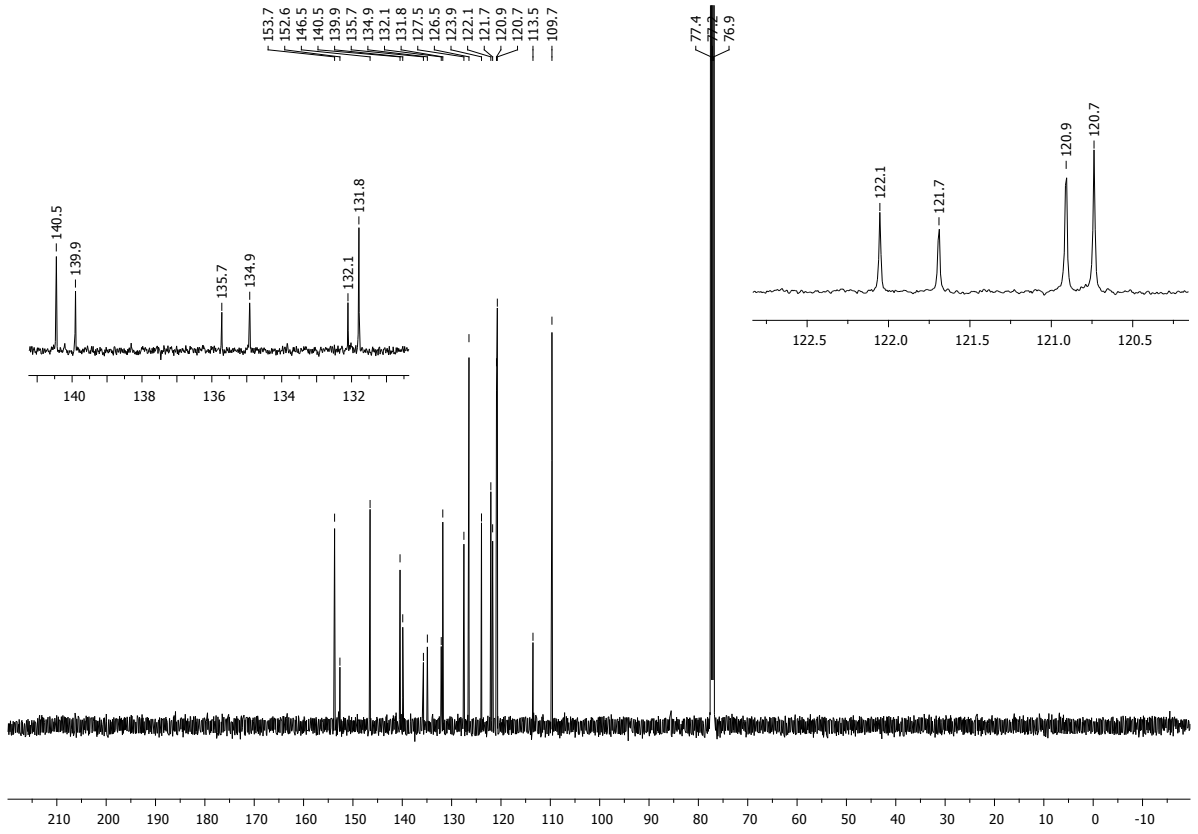

9-[4-(9*H*-Carbazol-9-yl)phenyl]-9*H*-purine-6-carbonitrile (PCBz-2)

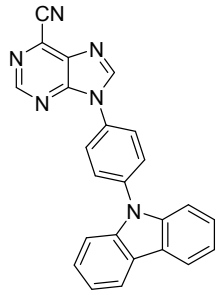

Synthesized according to general method B: compound **2b** (250 mg, 0.63 mmol, 1.0 eq.), sodium methanesulfinate salt (64 mg, 0.63 mmol, 1.0 eq.), KCN (82 mg, 1.26 mmol, 2.0 eq.), dry DMF (8 mL), 1 h, 80 °C. Silica gel column chromatography (DCM/MeCN, gradient 0% → 2%) provided product **PCBz-2** (yield: 138 mg, 57%) as a pale yellow solid. R_f = 0.57 (DCM/MeCN = 20:1). m. p. = 260–262 °C (crystalized form DCM/MeOH). HPLC: t_R = 6.94 min, eluent E_1. IR (KBr) ν (cm^{-1}): 3063, 2236, 1587, 1524, 1454, 1337, 1222. ^{1}H-NMR (500 MHz, $CDCl_3$) δ (ppm): 9.20 (s, 1H, H-C(2)), 8.67 (s, 1H, H-C(8)), 8.17 (d, 2H, ^3J = 7.6 Hz, 2×H-C(Ar)), 7.99 (d, 2H, ^3J = 8.4 Hz, 2×H-C(Ar)), 7.88 (d, 2H, ^3J = 8.4 Hz, 2×H-C(Ar)), 7.52 (d, 2H, ^3J = 7.6 Hz, 2×H-C(Ar)), 7.46 (t, 2H, ^3J = 7.6 Hz, 2×H-C(Ar)), 7.35 (t, 2H, ^3J = 7.6 Hz, 2×H-C(Ar)). ^{13}C-NMR (126 MHz, $CDCl_3$) δ (ppm): 153.7, 152.7, 146.8, 140.6, 139.0, 135.7, 132.1, 132.0, 128.8, 126.4, 125.2, 123.9, 120.8, 120.7, 113.5, 109.6. HRMS (ESI) m/z: $[M+H]^+$ Calcd for $C_{24}H_{15}N_6$ 387.1353; Found 387.1334.

^{1}H-NMR (500 MHz, $CDCl_3$) spectrum of compound PCbz-2:

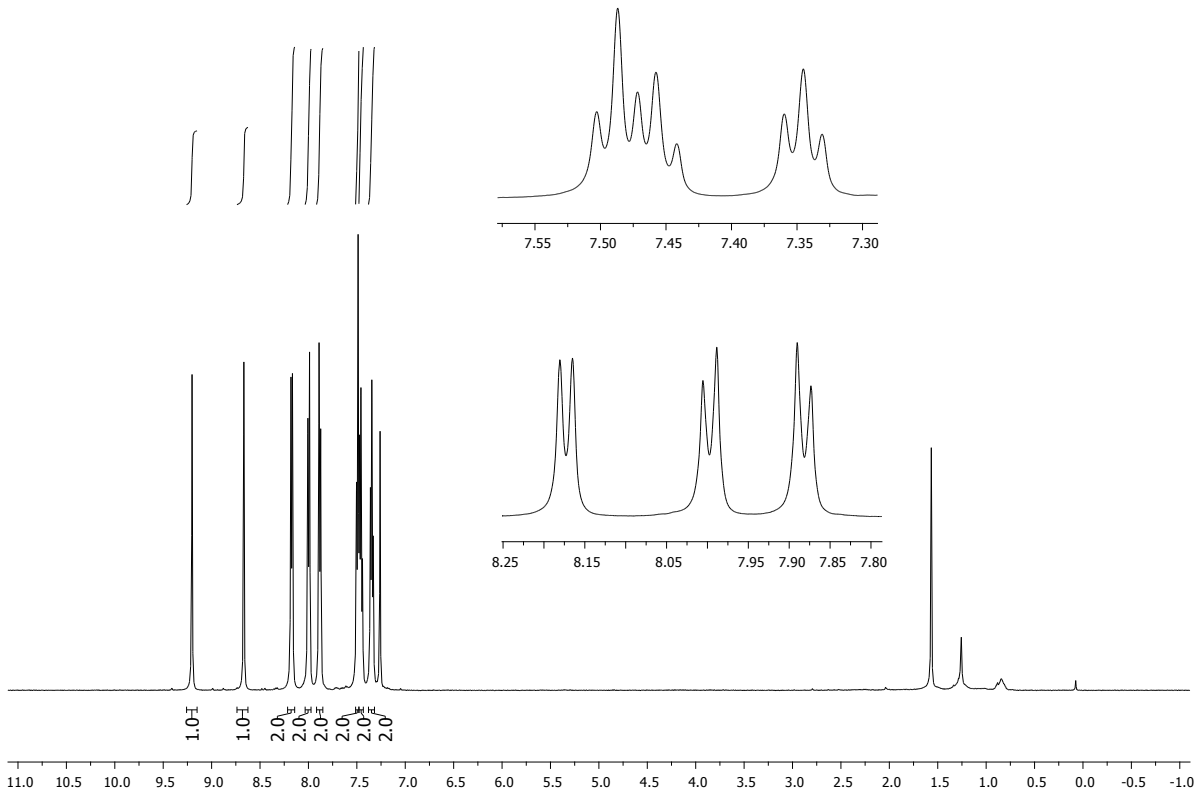

^{13}C-NMR (126 MHz, $CDCl_3$) spectrum of compound PCbz-2:

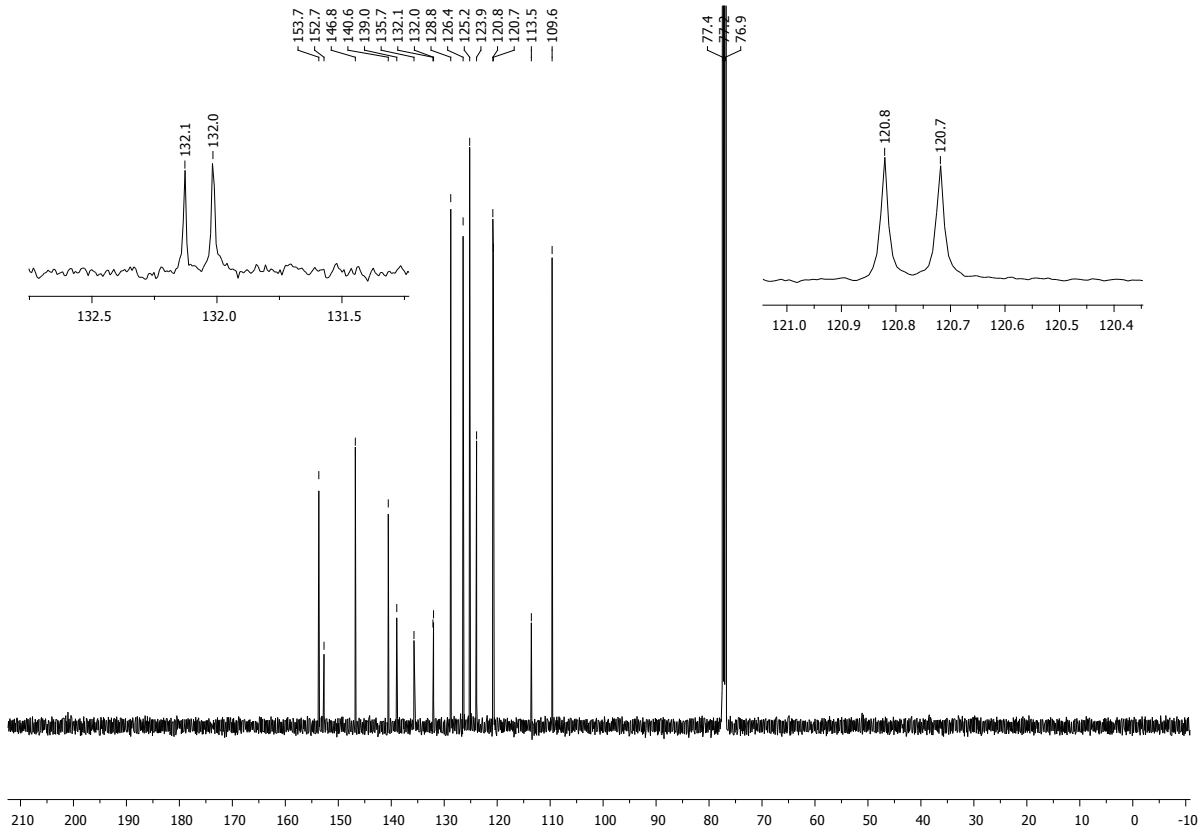

9-[3,5-Di(9*H*-carbazol-9-yl)phenyl]-9*H*-purine-6-carbonitrile (PCbz-3)

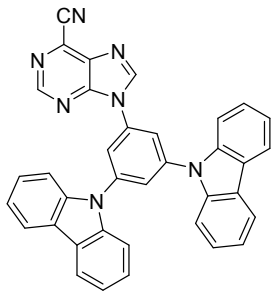

Synthesized according to general method B: Compound **3c** (250 mg, 0.45 mmol, 1.0 eq.), sodium methanesulfinate salt (45 mg, 0.45 mmol, 1.0 eq.), KCN (58 mg, 0.90 mmol, 2.0 eq.), dry DMF (5 mL), 1 h, 80 °C. Silica gel column chromatography (DCM/MeCN, gradient 0% → 2%) provided product **PCbz-3** (yield: 127 mg, 51%) as a pale yellow solid. R_f = 0.70 (DCM/MeCN = 20/1). HPLC: t_R = 6.91 min, eluent E_2. IR (KBr) ν (cm^{-1}): 3077, 2249, 1601, 1586, 1464, 1441, 1331, 1226. ^{1}H-NMR (500 MHz, $CDCl_3$) δ (ppm): 9.19 (s, 1H, H-C(2)), 8.70 (s, 1H, H-C(8)), 8.21–8.14 (m, 6H, 6×H-C(Ar)), 8.06–8.03 (m, 1H, H-C(Ar)), 7.68 (d, 4H, ^3J = 8.3 Hz, 4×H-C(Ar)), 7.49 (t, 4H, ^3J = 7.6 Hz, 4×H-C(Ar)), 7.36 (t, 4H, ^3J = 7.6 Hz, 4×H-C(Ar)). ^{13}C-NMR (126 MHz, $CDCl_3$) δ (ppm): 153.9, 152.6, 146.1, 141.4, 140.2, 136.1, 135.8, 132.3, 126.7, 124.9, 124.2, 121.3, 120.9, 119.6, 113.4, 109.7. HRMS (ESI) m/z: $[M+H]^+$ Calcd for $C_{36}H_{22}N_7$ 552.1931; Found 552.1911.

^{1}H-NMR (500 MHz, $CDCl_3$) spectrum of compound PCbz-3:

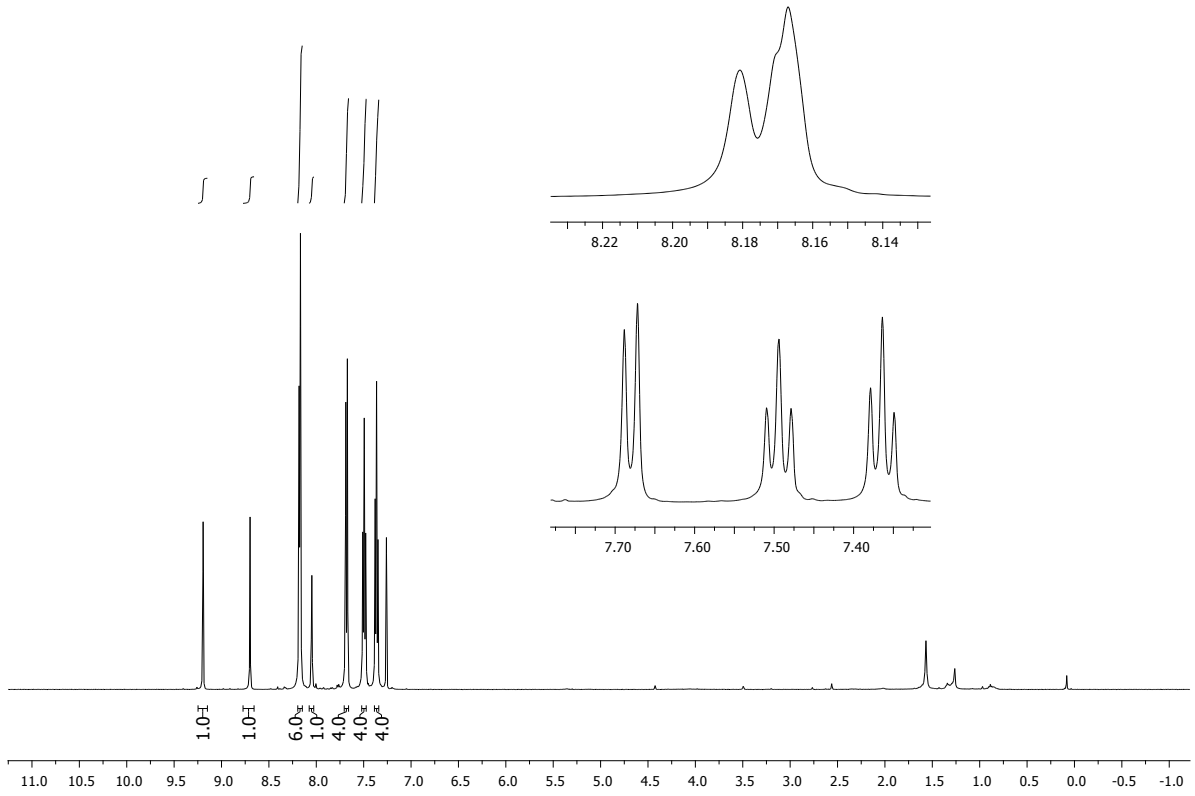

^{13}C-NMR (126 MHz, $CDCl_3$) spectrum of compound PCbz-3:

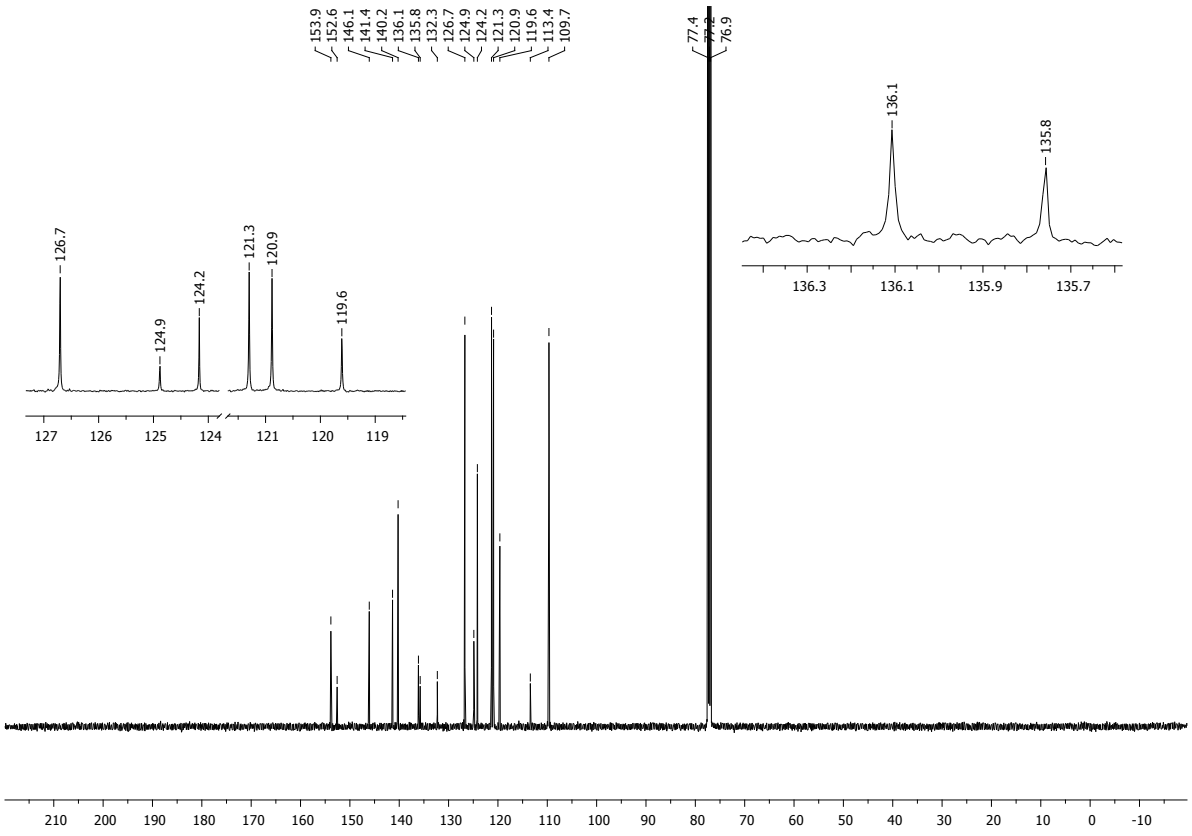
153.9
152.6
146.1
141.4
140.2
136.1
135.8
132.3
126.7
124.9
124.2
121.3
120.9
119.6
113.4
109.7
77.4
76.9
126.7
124.9
124.2
121.3
120.9
119.6
127
126
125
124
121
120
119
136.1
135.8
136.3
136.1
135.9
135.7
210
200
190
180
170
160
150
140
130
120
110
100
90
80
70
60
50
40
30
20
10
0
-10

References

1 F. B. Dias, T. J. Penfold and A. P. Monkman, *Methods Appl. Fluoresc.*, 2017, **5**, 012001.

2 J. Latvels, R. Grzibovskis, K. Pudzs, A. Vembris and D. Blumberga, eds. B. P. Rand, C. Adachi, D. Cheyns and V. van Elsbergen, 2014, p. 91371G.

3 F. Neese, *WIREs Comput. Mol. Sci.*, 2018, **1**, e1327.

4 M. D. Hanwell, D. E. Curtis, D. C. Lonie, T. Vandermeersch, E. Zurek and G. R. Hutchison, *J. Cheminform.*, 2012, **4**, 17.

5 T. Yanai, D. P. Tew and N. C. Handy, *Chem. Phys. Lett.*, 2004, **393**, 51–57.

6 A. D. Bochevarov, E. Harder, T. F. Hughes, J. R. Greenwood, D. A. Braden, D. M. Philipp, D. Rinaldo, M. D. Halls, J. Zhang and R. A. Friesner, *Int. J. Quantum Chem.*, 2013, **113**, 2110–2142.

7 H. S. Yu, X. He, S. L. Li and D. G. Truhlar, *Chem. Sci.*, 2016, **7**, 5032–5051.